PL-TR-92-2118

CONTINUOUS SEISMIC THRESHOLD MONITORING OF THE NORTHERN NOVAYA ZEMLYA TEST SITE; LONG-TERM OPERATIONAL CHARACTERISTICS

T. Kvaerna

NTNF/NORSAR
Post Box 51
N-2007 Kjeller, NORWAY

28 February 1992

Scientific Report No. 12

PHILLIPS LABORATORY
AIR FORCE SYSTEMS COMMAND
HANSCOM AIR FORCE BASE, MASSACHUSETTS 01731-5000

SPONSORED BY
Defense Advanced Research Projects Agency
Nuclear Monitoring Research Office
ARPA ORDER NO. 5307

MONITORED BY
Phillips Laboratory
Contract No. F49620- 89-C-0038

The views and conclusions contained in this document are those of the authors and should not be interpreted as representing the official policies, either expressed or implied, of the Defense Advanced Research Projects Agency or the U.S. Government.

This technical report has been reviewed and is approved for publication.

JAMES F. LEWKOWICZ
Contract Manager
Solid Earth Geophysics Branch
Earth Sciences Division

JAMES F. LEWKOWICZ
Branch Chief
Solid Earth Geophysics Branch
Earth Sciences Division

DONALD H. ECKHARDT, Director
Earth Sciences Division

This report has been reviewed by the ESD Public Affairs Office (PA) and is releasable to the National Technical Information Service (NTIS).

Qualified requestors may obtain additional copies from the Defense Technical Information Center. All others should apply to the National Technical Information Service.

If your address has changed, or if you wish to be removed from the mailing list, or if the addressee is no longer employed by your organization, please notify PL/IMA, Hanscom AFB, MA 01731-5000. This will assist us in maintaining a current mailing list.

Do not return copies of this report unless contractual obligations or notices on a specific document requires that it be returned.

REPORT DOCUMENTATION PAGE

Form Approved
OMB No. 0704-0188

1. AGENCY USE ONLY *(Leave blank)*	2. REPORT DATE	3. REPORT TYPE AND DATES COVERED
	28 February 1992	Scientific Report No. 12

4. TITLE AND SUBTITLE
Continuous Seismic Threshold Monitoring of the Northern Novaya Zemlya Test Site; Long-Term Operational Characteristics

5. FUNDING NUMBERS
PE 62714E
PR 9A10 TA DA WU BH

Contract F49620-89-C-0038

6. AUTHOR(S)
T. Kvaerna

7. PERFORMING ORGANIZATION NAME(S) AND ADDRESS(ES)
NTNF/NORSAR
Post Box 51
N-2007 Kjeller, NORWAY

8. PERFORMING ORGANIZATION REPORT NUMBER

9. SPONSORING/MONITORING AGENCY NAME(S) AND ADDRESS(ES)
Phillips Laboratory
Hanscom AFB, MA 01731-5000

Contract Manager: James Lewkowicz/GPEH

10. SPONSORING/MONITORING AGENCY REPORT NUMBER
PL-TR-92-2118

11. SUPPLEMENTARY NOTES

12a. DISTRIBUTION/AVAILABILITY STATEMENT
Approved for public release; distribution unlimited

12b. DISTRIBUTION CODE

13. ABSTRACT *(Maximum 200 words)*

In this work we demonstrate the practical capability of the Continuous Seismic Threshold Monitoring method to monitor the northern Novaya Zemlya test site at a very low threshold over an extended time period, using data from the Fennoscandian array network (NORESS, ARCESS and FINESA). We show that during February 1992 the network based magnitude threshold, at the 90% confidence level, stays below $m_b = 2.50$, 99.72% of the total time. We further "explain" all peaks in the network magnitude thresholds exceeding $m_b = 2.6$ as resulting from interfering signals from an identified seismic event (teleseismic or regional), or a short outage of the most important array (ARCESS). We also argue that this implies that at the given confidence level, there has been no seismic event of $m_b \geq 2.6$ at the northern Novaya Zemlya test site during February 1992.

During normal conditions, i.e., when the network threshold is low, ARCESS is clearly the most important array, followed by NORESS and FINESA. But during time periods when the ARCESS noise level is high, or when there are interfering events, the relative contribution of NORESS and FINESA increases significantly. The redundancy resulting from the use of several arrays is also essential during outages of one or more of the arrays.

14. SUBJECT TERMS	15. NUMBER OF PAGES
Seismic threshold monitoring Novaya Zemlya test site Fennoscandian regional array network	60
	16. PRICE CODE

17. SECURITY CLASSIFICATION OF REPORT	18. SECURITY CLASSIFICATION OF THIS PAGE	19. SECURITY CLASSIFICATION OF ABSTRACT	20. LIMITATION OF ABSTRACT
Unclassified	Unclassified	Unclassified	SAR

The threshold magnitudes for each array during background noise conditions are close to normally distributed, at least within shorter time intervals. Small deviations from the normal distribution occur because of long-term fluctuations in the background noise level. The average magnitude thresholds at FINESA exhibit strong weekly and diurnal variations. The latter are particularly significant on workdays. The average NORESS thresholds show rather small variations, whereas at ARCESS, large variations of more than 0.5 m_b units are observed. The causes of the peak periods at ARCESS are most likely severe wind and weather conditions.

Preface

Under Contract No. F49620-C-89-0038, NTNF/NORSAR is conducting research within a wide range of subjects relevant to seismic monitoring. The emphasis of the research program is on developing and assessing methods for processing of data recorded by networks of small-aperture arrays and 3-component stations, for events both at regional and teleseismic distances. In addition, more general seismological research topics are addressed.

Each quarterly technical report under this contract presents one or several separate investigations addressing specific problems within the scope of the statement of work. Summaries of the research efforts within the program as a whole are given in annual technical reports.

This Scientific Report No. 12 presents a manuscript entitled "Continuous seismic threshold monitoring of the northern Novaya Zemlya test site; long-term operational characteristics" by T. Kværna.

NORSAR Contribution No. 458

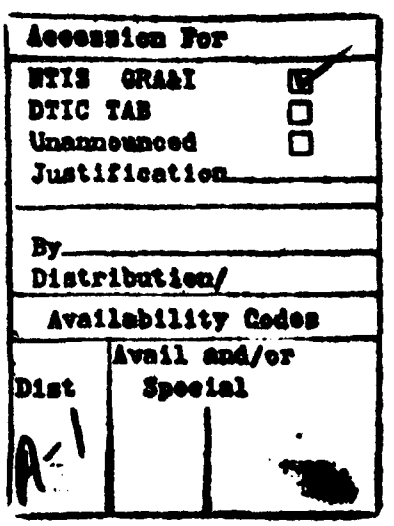

Continuous seismic threshold monitoring of the northern Novaya Zemlya test site; long-term operational characteristics

by

Tormod Kværna

NTNF/NORSAR
P.O. Box 51
N-2007 Kjeller, NORWAY

Abstract

In this work we demonstrate the practical capability of the Continuous Seismic Threshold Monitoring method to monitor the northern Novaya Zemlya test site at a very low threshold over an extended time period, using data from the Fennoscandian array network (NORESS, ARCESS and FINESA). We show that during February 1992 the network based magnitude threshold, at the 90% confidence level, stays below $m_b = 2.50$, 99.72% of the total time. We further "explain" all peaks in the network magnitude thresholds exceeding $m_b = 2.6$ as resulting from interfering signals from an identified seismic event (teleseismic or regional), or a short outage of the most important array (ARCESS). We also argue that this implies that at the given confidence level, there has been no seismic event of $m_b \geq 2.6$ at the northern Novaya Zemlya test site during February 1992.

During normal conditions, i.e., when the network threshold is low, ARCESS is clearly the most important array, followed by NORESS and FINESA. But during time periods when the ARCESS noise level is high, or when there are interfering events, the relative contribution of NORESS and FINESA increases significantly. The redundancy resulting from the use of several arrays is also essential during outages of one or more of the arrays.

The threshold magnitudes for each array during background noise conditions are close to normally distributed, at least within shorter time intervals. Small deviations from the normal distribution occur because of long-term fluctuations in the background noise level. The average magnitude thresholds at FINESA exhibit strong weekly and diurnal variations. The latter are particularly significant on workdays. The average NORESS thresholds show rather small variations, whereas at ARCESS, large variations of more than 0.5 m_b units are observed. The causes of the peak periods at ARCESS are most likely severe wind and weather conditions.

Introduction

The theoretical background for and applications of the continuous seismic threshold monitoring metod (CSTM) have been described in several articles. The approach was introduced by Ringdal and Kværna (1989), who showed that by continuously monitoring the seismic amplitude level at several seismic stations or arrays, one can at any time obtain an instant network-based magnitude threshold for a given target region. The magnitude threshold can be interpreted as the maximum magnitude of a possible clandestine explosion, given a predefined level of confidence. In the context of a comprehensive or threshold test ban treaty, the continuous assessment of the magnitude thresholds makes it possible to focus attention upon those specific time intervals when realistic evasion opportunities exist, while retaining confidence that no treaty violation has occurred at other times.

Kværna and Ringdal (1990) presented results from a one-week experiment of continuously monitoring the northern Novaya Zemlya test site. Data from the Fennoscandian regional array network (ARCESS, FINESA, and NORESS), see Fig. 1, were used to calculate the magnitude thresholds. It was found that the test site could be consistently monitored at a very low magnitude level (typically $m_b = 2.5$). In fact, every occurrence of the threshold exceeding $m_b = 2.5$ could be explained as resulting from an identified interfering event signal either at teleseismic or regional distance.

The excellent capability of the Fennoscandian regional array network to monitor the northern Novaya Zemlya test site was further confirmed by an experiment where recordings of the Novaya Zemlya nuclear test of October 24, 1990 were downscaled to $m_b = 2.6$ and superimposed on different noise intervals (Kværna, 1991).

In the context of using CSTM as a tool in routine monitoring, it is important to determine how the method will work under different conditions. Variability in the seismic noise level, occurrences of large earthquakes and aftershock sequences, station downtimes and data quality problems are all factors that will influence the performance of CSTM. Again focusing on the northern Novaya Zemlya test site, using data from the Fennoscandian regional array network, we have analyzed one month of magnitude threshold data (February, 1992) for the purpose of evaluating the long-term operational characteristics of CSTM.

Analysis of network threshold peaks

Our monitoring experiment was conducted in the same way and with the same parameter settings as used by Kværna and Ringdal (1990), and we have also in this study chosen to present the monitoring results in terms of plots covering one data day each. In Figs. A-1 to A-29 of the Appendix, each covering one day of February, 1992, we have identified all time periods where the network magnitude thresholds at the 90% confidence level exceed $m_b = 2.6$.

For the remainder of this paper, the term magnitude threshold implies the magnitude threshold at the 90% confidence level.

From investigation of the distribution of all network CSTM data (totally 696 hours for February, 1992), we found that the network magnitude threshold exceeded

$m_b = 2.6$ for about 50 minutes, see Fig. 2. This is only 0.12% of the total time, and we found $m_b = 2.6$ to be a suitable magnitude limit, in the sense that we were able to identify all interfering event signals causing the threshold to exceed this limit. One might of course argue that we should instead attempt to explain all peaks exceeding $m_b = 2.5$, but with reference to the actual CSTM data, we found that there were several intervals with m_b between 2.5 and 2.6, which we were not able to account for by signals from identified events. These intervals were all characterized either by a high background noise level at ARCESS, or with gaps in the ARCESS recordings.

The upper three traces of each figure of the Appendix represent the magnitude thresholds obtained from the three indivitual arrays, whereas the bottom trace illustrates the network threshold. Typically, the individual array traces have a number of significant peaks for each 24-hour period, due to signals from interfering events (regional or teleseismic). On the network trace, the number and sizes of these peaks are significantly reduced, because an interfering event usually will not provide matching signals at all stations. From probabilistic considerations, it can in such cases be inferred that the actual network threshold is lower than these individual peaks might indicate.

Data gaps or data quality problems are indicated by dropouts or gaps on the individual array traces. Obviously, during these intervals, the affected array did not contribute to the network threshold estimates.

On each of the one-day figures of the Appendix, the arrows indicate peaks with network magnitude threshold exceeding $m_b = 2.6$. A few peaks with slightly lower thresholds are also marked. A **T** at the arrow indicates that the peak is caused by signals from a teleseismic event, whereas an **R** indicates signals from a regional or local event. On three different occasions the threshold slightly exceeded 2.6 due to gap in the ARCESS recordings. These peaks are indicated by a **G** at the arrows.

A summary of the threshold peaks and the events causing the peaks is given in Table 1. Following the definition of the CSTM peaks (i.e., date, time, magnitude threshold, and number of seconds with the threshold exceeding $m_b = 2.6$), there is a bulletin of the events causing the peaks in the magnitude threshold traces. From Table 1 it can be seen that in some cases more than one event is contributing to the same peak in the threshold trace.

During the first half of February, there were several large teleseismic events causing increases in the network threshold (see events reported by the Quick Epicenter Determinations (QED) of the USGS), whereas during the second half of February, almost all CSTM peaks were caused by regional events. The regional events were all processed and located by the Intelligent Monitoring System (IMS) (Bache et al., 1990). The epicenters of the regional events of Table 1 are plotted on the map of Fig. 3. Except for one felt earthquake in southern Norway ($M_L = 3.26$), the events are most likely mining explosions, as their epicenters coincide with known mining sites. Within the context of practical monitoring, it is interesting that for a 5-day period (February 23 through 27) there were no threshold peaks exceeding $m_b = 2.6$.

Continuous thresholds during noise conditions

For the purpose of analyzing the long-term fluctuations of the magnitude thresholds, we have for every 4-hour interval computed the median thresholds. The robust median estimator has been chosen to ensure that we are minimizing the influence of the short-term event peaks. These statistics have been computed for the network and for each array separately. The thresholds are all derived from filtered array beams, and thereby reflect the noise fluctuations within the applied frequency bands. The frequency filters used for ARCESS, FINESA and NORESS are 3.0-5.0 Hz, 2.0-4.0 Hz and 1.5-3.5 Hz, respectively.

Fig. 4a illustrates the results for each array for the month of February. It is clearly seen that ARCESS (the lower dashed line) has the best average capability for monitoring the northern Novaya Zemlya test site. Except for a few short time intevals, ARCESS has on the average lower magnitude thresholds than any of the other two arrays (NORESS - solid line, FINESA - upper dashed line). The ARCESS threshold curve has five pronounced peaks during the month, and shows internal variations of more than 0.5 m_b units. During quiet noise conditions, the median magnitude thresholds fluctuate around $m_b = 2.0$, but during the high-noise periods the thresholds approaches $m_b = 2.5$. Two of the peaks have been verified to correlate with severe wind and weather conditions in the ARCESS region, and it is also likely that the other three peaks are weather generated.

Compared to ARCESS, the NORESS magnitude thresholds show rather small variations, and fluctuate between m_b 2.4 and 2.5 during the entire period, see Fig. 4a. The small diurnal variations (of the order of 0.1 m_b units), are consistent with the findings of Fyen (1990). He found that for frequencies below 2 Hz, there was little difference between daytime and nighttime noise levels, whereas at higher frequencies, the diurnal variations are more significant (0.2-0.3 m_b units). It is only for a short time interval on February 8 that NORESS on the average has the best monitoring capability of the three arrays, but it has to be emphasized that this is not necessarily representative for time periods when seismic signals are present.

The median magnitude thresholds of FINESA, given by the top dashed line of Fig. 4a, exhibit strong weekly and diurnal variations. The diurnal variations are particularly significant on workdays. One peak for each of the five workdays are followed by a quiet weekend, reflecting the relative behavior of the background noise field in the frequency band of the P-beam steered towards Novaya Zemlya (2.0-4.0 Hz). The median thresholds during the weekends are approaching that of NORESS, whereas the workday levels are 0.2 to 0.4 m_b units higher. ¿From Fig. 4a it can thus be inferred that FINESA on the average is contributing less than the other two arrays to the network monitoring capability of the northern Novaya Zemlya test site, but again, this may not be representative for time periods when seismic signals are present.

In Fig. 4b, we compare the median network performance (solid line) and the median ARCESS performance (dashed line) for monitoring the northern Novaya Zemlya test site. It is seen that when the ARCESS thresholds are low, the two curves almost coincide, implying that ARCESS alone determines the average network monitoring performance. However, during the ARCESS peak periods, the network curve is

lower. This shows that even during background noise conditions, the other two arrays (FINESA and NORESS) contribute to lowering the magnitude thresholds.

We have in this section discussed the average properties of the CSTM performance of the Fennoscandian array network for monitoring the northern Novaya Zemlya test site. We have concluded that for most of the time, ARCESS is the array with the best capability, but that the other two arrays also play an important role, particularly when the ARCESS noise level is high.

The performance during time intervals with event signals can not be decribed by this approach, and it is necessary to devise a method that highlights the behavior of the extremes of the CSTM data distribution. This will be done in the following section.

Continuous thresholds during intervals with interfering signals

The CSTM data can be regarded as a distribution containing elements from a background noise field and a signal field. Fig. 5 shows so-called quantile plots of a nighttime interval without any strong events (February 27, 00:00 - 04:00). If the data points of a normal quantile plot fit with a straight line, the data follow a normal distribution. It can be seen from Fig. 5 that except for the higher extrema of the distributions, the CSTM data for the network and the individual arrays are close to normally distributed. From this it can be inferred that the background noise field can be approximated by a normal distribution, at least within shorter time intervals. The anomalous higher extrema are the effect of event signals. This is further confirmed by the quantile plots of a daytime interval with many events (Feb. 26, 10:00 - 14:00), see Fig. 6. In this case, a larger fraction of the data, at the higher end of the distribution, deviates from the normal. This is particularly striking at FINESA, which has a very large number of event peaks in the CSTM data during this time interval, see Fig. A-26. It should also be noted that at the lower magnitudes, the quantile plots of ARCESS and the network are almost similar, but at the higher extrema, the network magnitudes are lower. This illustrates that in cases where the best array of the network (i.e., ARCESS) has high threshold magnitudes, data from the other arrays are critical for lowering the network magnitude thresholds.

The dramatic improvement in the practical monitoring capability when using a network of arrays instead of a single array is illustrated in Fig. 7. We have for the month analyzed counted the number of threshold peaks exceeding a given magnitude, both for the network and for the best array (ARCESS). The barplots of Fig. 7 show that at a threshold of 2.6, the number of network threshold peaks are reduced by a factor of five in comparison to the threshold peaks at ARCESS alone (i.e., from 293 to 56). At a threshold of 3.0 the improvement is better than a factor of ten (i.e., from 41 to 3).

The CSTM method treats the individual phase thresholds as independent observations. ¿From probabilistic considerations, it can be inferred that the actual network threshold is lower than any of the individual phase thresholds might indicate. Details on this procedure are given by Ringdal and Kværna (1989). Let us assume that we

have a phase magnitude observation of $m_b = 2.5$ with an assumed standard deviation of 0.2. In this case the 90% threshold is $m_b = 2.76$. But if we had two such observations of $m_b = 2.5$, and assuming independence, the 90% combined network threshold would be $m_b = 2.60$.

Let us consider the case of two magnitude observations in more detail. Fig. 8 shows the improvement of the combined thresholds as a function of the magnitude difference between the two observations. This illustrates that if a phase magnitude observation is close to the lowest one of the network, it will contribute significantly to lowering the network threshold. Table 2 gives the total time for which the threshold of each of the arrays was within 0.3 m_b units of the best array of the network. From Fig. 8 it can be seen that a difference of 0.3 is tied to a network improvement of 0.05 m_b units. From Table 2 it is clear that ARCESS and NORESS play a very important role in lowering the network thresholds for the northern Novaya Zemlya test site, whereas the contribution from FINESA is less during normal noise conditions.

However, the relative contributions from the three arrays change significantly when the network threshold is high, i.e., during intervals with event signals. Table 3 show a statistic similar to that of Table 2, but only considering intervals when the network threshold exceed 2.6. We find that NORESS and FINESA become much more important and that ARCESS no longer plays such a dominant role. These results are in accordance with those shown in Fig. 7

In practical operation of any seismic network, there will from time to time be intervals where data from one or more stations are missing, e.g., caused by hardware or communication problems. Under such circumstances, it is important the we have a sufficiently large number of stations in our network, so that we even without these data retain usable magnitude thresholds. For the time period analyzed, we had very few data gaps (see Table 4), and it never occurred that two or more arrays were missing data simultaneously. But if data from ARCESS were missing for a longer time period, the availability of data from FINESA would be critical for the CSTM operation. We found that during normal conditions, the FINESA threshold was within 0.3 m_b units of the best array 2.64% of the time, but if we only compare to NORESS (assuming missing ARCESS data), this percentage for the month of February increases to 51.40.

Conclusions

This work has documented the practical capability of the Continuous Seismic Threshold Monitoring method to monitor a specific nuclear test site at a very low threshold over an extended time period.

Specifically, we have used the Fennoscandian array network (NORESS, ARCESS and FINESA) to monitor the northern Novaya Zemlya test site for one full month (February 1992). We have shown that the magnitude threshold stays below $m_b = 2.50$ 99.72% of the total time. We have further "explained" all of the peaks exceeding $m_b = 2.6$ as resulting from one of the following three conditions: 1) a "large" identified teleseismic event, 2) a "large" identified regional event and 3) a short outage of the most important array (ARCESS).

The natural question is then as follows: Do these results imply that at the given confidence level there has been no seismic event of $m_b \geq 2.6$ at the test site during February 1992?

The answer is in practice "yes", since such an event only could have occurred during one of the time intervals when the network threshold trace exceeds 2.6. We have noted that the combined time span of such exceedances was only 50 minutes, or 0.12% of the total time. Since all the peaks were explained as resulting from known causes, it seems extremely unlikely that an event of $m_b \geq 2.6$ actually occurred during one of these short event intervals.

In theory, in a hypothetical monitoring situation for a comprehensive test ban treaty, there might be an "evasion" possibility if any of such high threshold periods could be predicted. But we do not consider this to be a realistic scenario. First, such predictions require exact knowledge of the configuration and the performance of the monitoring network, and second, there are a lot of practical problems involved in carrying out such a clandestine explosion so that the probability of getting detected is very high.

We have studied the relative contributions of the three arrays and found that ARCESS is clearly the most important, followed by NORESS and FINESA. During time periods when the ARCESS noise level is high, or when there are interfering events, the relative contributions of NORESS and FINESA increase significantly. The redundancy created by using several arrays is also essential during outages of one or more of the arrays.

During background noise conditions, the threshold magnitudes for each array are close to normally distributed, at least within shorter time intervals. Small deviations from the normal distribution occur because of long-term fluctuations in the background noise level. The average magnitude thresholds at FINESA exhibit strong weekly and diurnal variations. The latter are particularly significant on workdays. The average NORESS thresholds show rather small variations, whereas at ARCESS, internal differences of more than 0.5 m_b units are observed. The peak periods at ARCESS are most likely caused by severe wind and weather conditions.

In the near future, additional array stations are planned for installation in the Arctic region. These stations would contribute to further improving the CSTM capability, both for Novaya Zemlya and on a general regional basis. This will be the subject for additional studies in the future.

REFERENCES

Bache, T., S. R. Bratt, J. Wang, R. M. Fung, C. Kobryn and J. W. Given (1990), The Intelligent Monitoring System, *Bull. Seism. Soc. Am.* 80, Part B, 1833-1851.

Fyen, J. (1990): Diurnal and seasonal variations in the microseismic noise level observed at the NORESS array, *Phys. Earth Planet. Inter.* 63, 252-268.

Kværna, T. and F. Ringdal (1990): Continuous threshold monitoring of the Novaya Zemlya test site, *Semiannual Tech. Summary, 1 Apr - 30 Sep 1990,* NORSAR Sci. Rep. 1-90/91, NORSAR, Kjeller, Norway.

Kværna, T (1991): Threshold monitoring of Novaya Zemlya: A scaling experiment, *Semiannual Tech. Summary, 1 Oct 1990 - 31 Mar 1991,* NORSAR Sci. Rep. 2-90/91, NORSAR, Kjeller, Norway.

Ringdal, F. and T. Kværna (1989): A multi-channel processing approach to real-time network detection, phase association, and threshold monitoring, *Bull. Seism. Soc. Am.* 79, 1927-1940.

Date	TM peak	Mag	Scc	Ev	Or. time	Lat	Lon	Dep	Mag	Bull	Region
02/01	11.46.11	2.66	20	R	11.46.08.8	67.592	30.300	0F	2.46	IMS	European Russia
02/01	19.12.06	2.99	88	T	19.04.05.3	35.164	139.702	107	5.6	QED	S.coast of Honshu
02/02	05.04.20	2.63	12	R	05.05.01.4	67.659	33.417	0F	2.41	IMS	European Russia
02/02	17.51.03	2.65	9	T	05.05.01.4	67.659	33.417	33F	5.5	QED	Kuril Islands
02/03	13.55.17	2.69	15	R	13.54.44.6	60.836	29.220	0F	2.41	IMS	European Russia
02/05	05.40.43	2.72	15	T	05.33.11.4	45.021	150.972	33F	5.6	QED	Kuril Islands
02/05	10.56.54	2.64	2	T	10.54.38.0	44.600	150.500	33F	4.3	NORSAR	Kuril Islands
02/05	13.21.09	2.90	69	T	13.13.42.5	52.163	-170.130	48	5.4	QED	Fox Islands
02/05	23.14.43	2.65	8	T	23.10.50.9	31.407	66.825	33F	5.1	QED	Afghanistan
02/06	01.23.52	2.95	181	T	01.12.41.2	-5.609	103.271	55	6.0	QED	Southern Sumatra
02/06	03.42.24	2.71	77	T	03.35.17.2	29.511	95.635	33F	5.6	QED	Xijang-India border
02/06	04.05.32	2.63	4	T	03.54.43.7	-5.374	103.197	72	5.5	QED	Southern Sumatra
02/06	05.13.26	2.63	3	T	04.57.28.0	-33.400	-175.200	33F	3.8	NORSAR	Kermadec Islands
02/06	09.19.03	2.78	39	R	09.18.47.9	61.243	29.875	0F	2.07	IMS	Finland-Russia border
				R	09.19.55.1	68.147	32.846	0F	1.90	IMS	European Russia
02/06	12.19.03	2.61	3	R	12.21.00.0	69.344	30.570	0F	2.14	IMS	Norway-Russia border
02/06	16.27.43	2.66	9	R	16.28.20.4	67.176	20.792	0F	1.83	IMS	Sweden
02/07	00.13.59	2.88	49	T	00.06.28.6	43.140	146.611	54	5.4	QED	Kuril Islands
02/07	06.42.13	2.67	20	T	06.35.26.0	52.925	159.555	49	5.3	QED	Off east coast of Kamchatka
02/07	08.38.36	2.66	15	R	08.41.05.1	67.633	33.715	0F	2.41	IMS	European Russia
02/07	09.20.39	2.61	1	R	09.21.16.4	68.190	32.875	0F	1.98	IMS	European Russia
				R	09.23.00.4	67.969	32.870	0F	1.92	IMS	European Russia
				R	09.25.08.3	59.298	26.399	0F	1.06	IMS	European Russia
02/07	09.54.59	2.65	15	T	09.48.38.7	55.795	160.753	138	5.0	QED	Kamchatka
02/07	09.59.36	2.64	5	R	10.00.44.9	64.692	30.728	0F	2.11	IMS	Finland-Russia border
02/07	12.18.59	2.80	21	R	12.20.52.2	69.329	30.842	0F	2.40	IMS	Norway-Russia border
02/08	11.44.28	2.69	29	R	11.44.41.2	67.648	30.594	0F	2.24	IMS	European Russia
02/09	04.09.14	2.63	5	R	04.09.41.1	67.574	33.741	0F	2.35	IMS	European Russia
02/09	07.56.42	2.57	-	T	07.49.21.5	51.497	-178.364	66	5.1	QED	Andreanof Islands
02/09	22.08.59	2.84	47	T	22.01.58.4	47.982	152.979	123	5.6	QED	Kuril Islands
02/12	01.09.22	2.82	42	T	01.02.01.9	51.299	177.926	33F	5.2	QED	Rat Islands
02/13	01.45.47	2.77	70	T	01.29.17.1	-15.923	166.215	33F	6.1	QED	Vanuatu Islands
02/13	02.45.31	2.82	54	T	02.38.18.4	53.576	-165.706	44	5.5	QED	Fox Islands
02/13	23.34.06	2.72	33	R	23.35.20.5	67.720	21.067	0F	1.84	IMS	Sweden
02/14	08.23.25	2.99	136	T	08.18.27.7	53.576	-165.706	33F	5.3	QED	Lake Baykal Region
02/14	08.48.02	2.61	1	R	08.48.20.2	67.391	32.939	0F	2.31	IMS	European Russia
02/14	12.19.23	2.96	115	R	12.21.00.9	69.322	30.727	0F	2.50	IMS	Norway-Russia border
02/15	11.47.38	2.62	1	R	11.49.21.2	67.656	30.374	0F	1.87	IMS	European Russia
02/15	12.57.21	2.76	61	T	12.52.55.0	42.846	46.588	33F	4.7	QED	Eastern Caucasus
02/16	08.49.11	2.70	27	R	08.49.50.5	67.636	33.547	0F	2.54	IMS	European Russia
02/16	21.55.47	2.53	-	R	21.54.36.6	67.667	20.841	0F	1.03	IMS	Sweden
02/17	00.04.52	3.13	136	T	00.01.56.7	79.190	124.625	10	5.8	QED	East of Severnaya Zemlya
02/17	08.13.48	2.65	27	G							Gap in ARCESS recording
02/17	14.23.57	2.71	33	R	14.25.24.0	69.638	30.430	0F	1.95	IMS	Norway-Russia border
02/17	15.45.13	2.63	4	G							Gap in ARCESS recording
02/18	12.42.04	2.68	8	R	12.42.01.9	59.337	27.065	0F	2.61	IMS	European Russia
02/19	06.40.25	2.91	226	R	06.39.32.9	59.240	10.886	0F	3.26	IMS	Southern Norway
02/19	12.26.49	3.25	302	R	12.25.03.0	69.257	30.575	0F	2.09	IMS	Norway-Russia border
				R	12.26.30.0	64.722	30.553	0F	2.78	IMS	Finland-Russia border
02/19	12.42.45	2.88	33	R	12.43.59.4	67.595	33.647	0F	2.46	IMS	European Russia
02/20	20.52.21	2.55	-	T	20.35.24.3	-33.498	-179.673	48	5.9	QED	South of Kermadec Islands
02/20	21.16.05	2.79	60	R	21.16.27.7	67.647	33.555	0F	1.98	IMS	European Russia
				R	21.16.50.5	67.918	33.951	0F	2.39	IMS	European Russia
02/21	08.59.39	2.74	103	R	08.59.25.1	67.657	33.791	0F	2.63	IMS	European Russia
02/21	11.01.46	3.14	173	R	11.01.53.5	64.672	30.801	0F	2.72	IMS	Finland-Russia border
02/21	12.49.06	2.99	135	R	12.50.11.2	69.341	30.688	0F	2.16	IMS	Norway-Russia border
				R	12.51.02.8	69.380	30.683	0F	2.46	IMS	Norway-Russia border
02/21	16.32.43	2.80	42	R	16.32.43.4	67.117	21.049	0F	2.02	IMS	Sweden
02/22	11.45.00	2.72	44	R	11.46.12.7	67.485	29.529	0F	1.87	IMS	Finland-Russia border
				R	11.46.59.0	67.558	30.328	0F	2.24	IMS	European Russia
02/22	11.59.31	2.70	35	R	12.00.18.7	67.599	33.659	0F	2.50	IMS	European Russia
02/28	08.58.22	2.75	36	R	08.58.59.1	67.617	33.769	0F	2.50	IMS	European Russia
02/28	12.07.37	2.63	2	R	12.09.56.9	59.170	27.332	0F	1.80	IMS	European Russia
02/28	12.19.10	2.69	37	G							Gap in ARCESS recording
02/28	12.43.14	2.92	243	R	12.45.11.0	69.365	30.647	0F	2.52	IMS	Norway-Russia border
02/28	14.30.16	2.68	17	R	14.30.29.5	67.709	33.695	0F	2.16	IMS	European Russia
				R	14.31.39.7	67.522	33.677	0F	2.31	IMS	European Russia

TABLE 1.

List of peaks in the network threshold traces and the events causing the peaks. Following the definition of the CSTM peaks (i.e., date, time, maximum magnitude threshold, and number of seconds with the threshold exceeding $m_b = 2.6$), there is a bulletin of the events causing the peaks in the magnitude threshold traces. It can be seen that in some cases more than one event is contributing to the same peak in the threshold trace.

Table 2

Station	Time within 0.3 of best array	% of total
ARCESS	28d 22h 16m 51s	99.75
NORESS	06d 00h 13m 25s	20.72
FINESA	18h 23m 38s	2.64

TABLE 2. Total time for which the threshold of each of the arrays was within 0.3 m_b units of the best array of the network.

Table 3

Station	Time within 0.3 of best array	% of total
ARCESS	36m 57s	73.97
NORESS	34m 04s	68.20
FINESA	07m 55s	15.85

TABLE 3. Total time for which the threshold of each of the arrays was within 0.3 m_b units of the best array of the network, but only considering intervals when the network threshold exceeded 2.6. For the month of February 1992 the network threshold exceeded 2.6 for 49 min. and 57 sec.

Table 4

Station	Time without data	% of total
ARCESS	32m 28s	0.06
NORESS	2h 00m 49s	0.29
FINESA	3h 36m 12s	0.52

TABLE 4. Total time without data for each of the arrays for the month of February 1992.

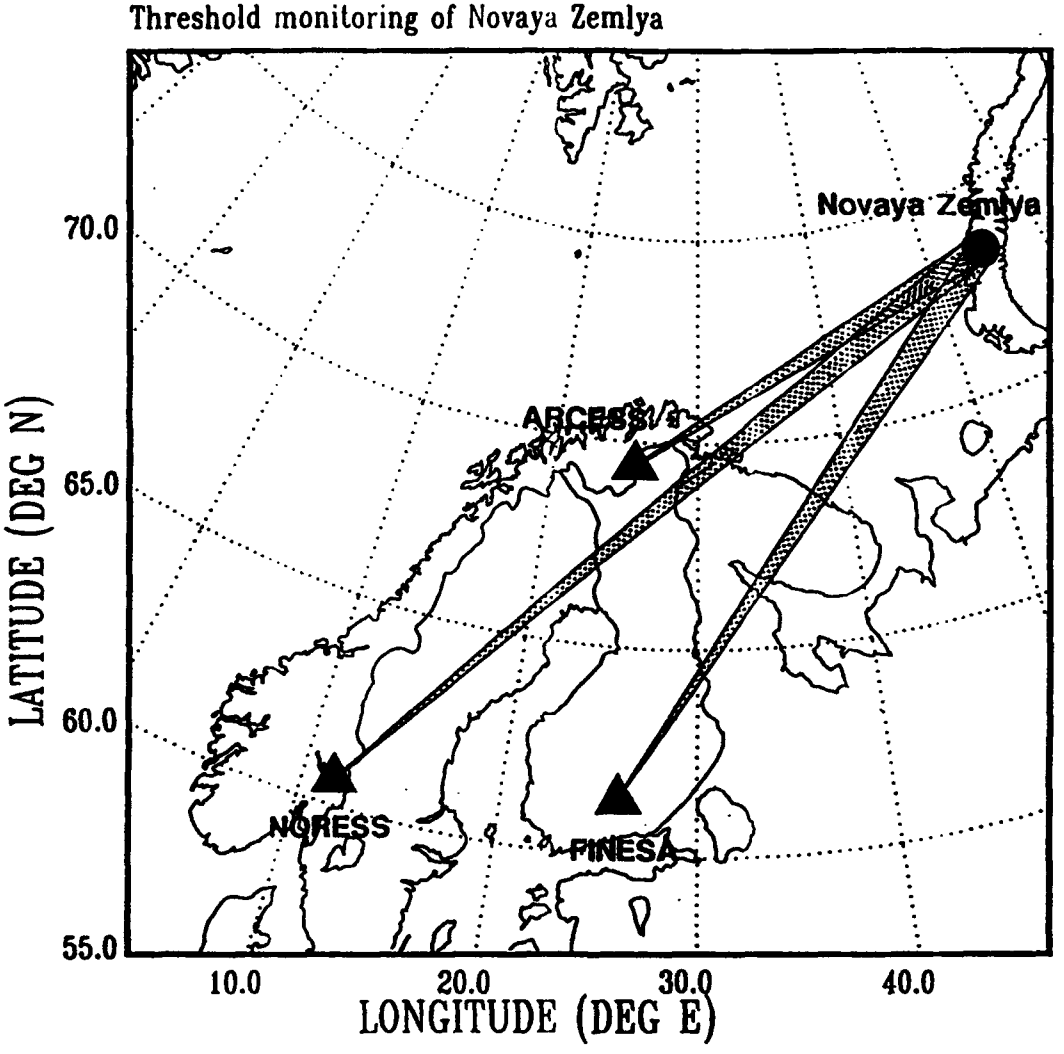

FIG. 1. Map showing the location of the northern Novaya Zemlya test site and the Fennoscandian array network. The distances of the three arrays from the test site are for NORESS 2280 km, for ARCESS 1100 km and for FINESA 1780 km.

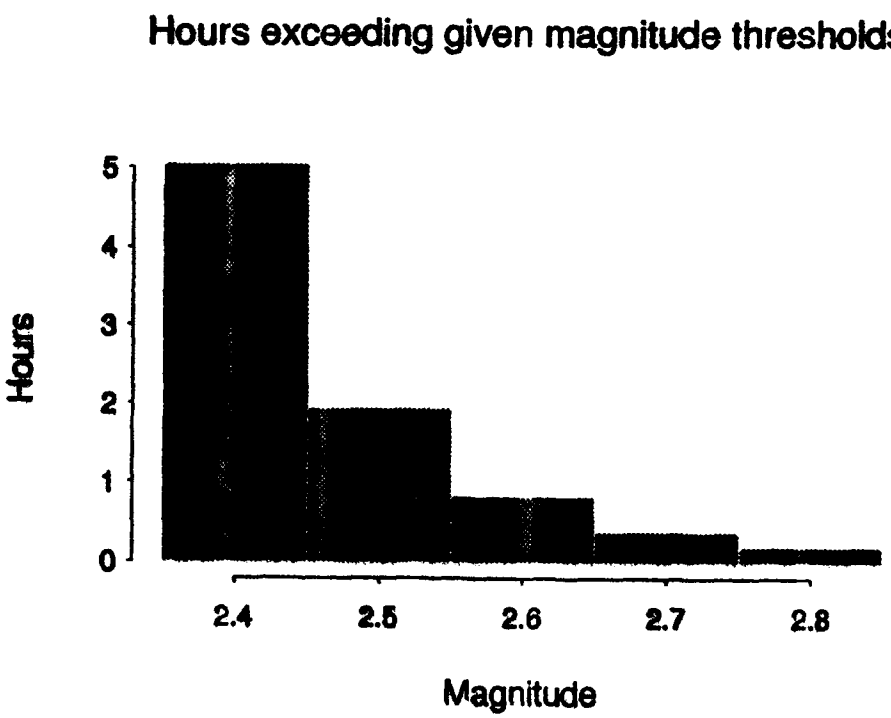

FIG. 2. Barplot showing the number of hours where the 90% network magnitude threshold exceeds a given magnitude, for the month of February, 1992.

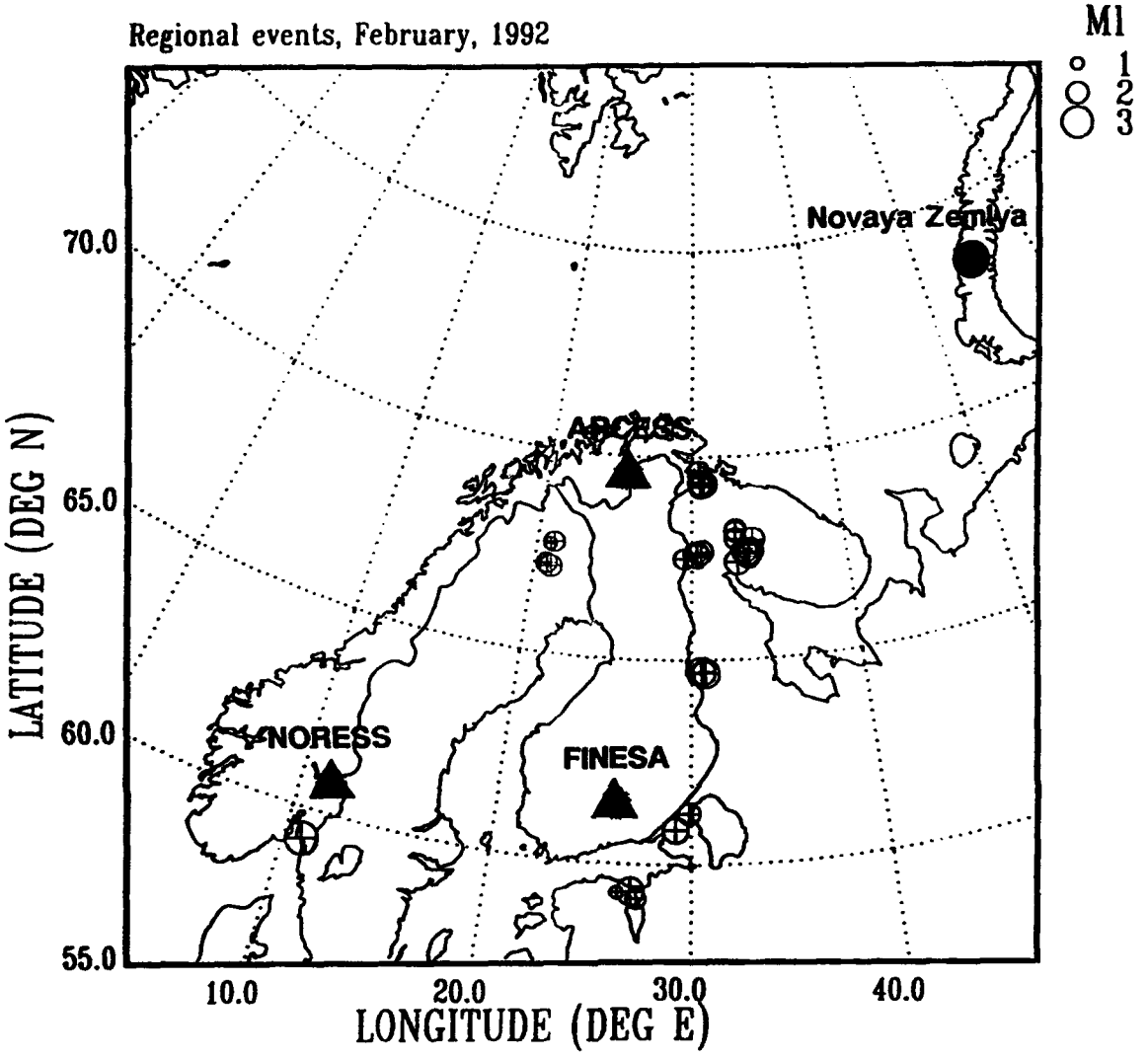

FIG. 3. Epicenters of regional events causing the network threshold to exceed m_b = 2.6. All events, except one felt earthquake in southern Norway are probable mining explosions. Note the large number of events on the Kola peninsula.

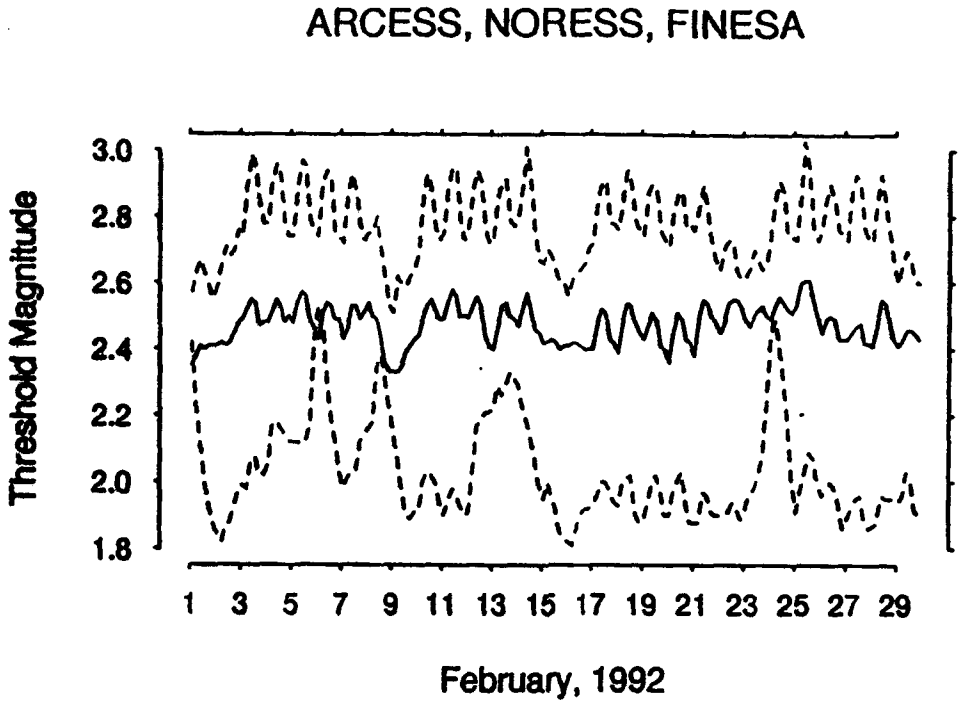

FIG. 4A.

Four-hour medians of the magnitude thresholds for each array for the month of February 1992.
Lower dashed line: ARCESS
Middle solid line: NORESS
Upper dashed line: FINESA

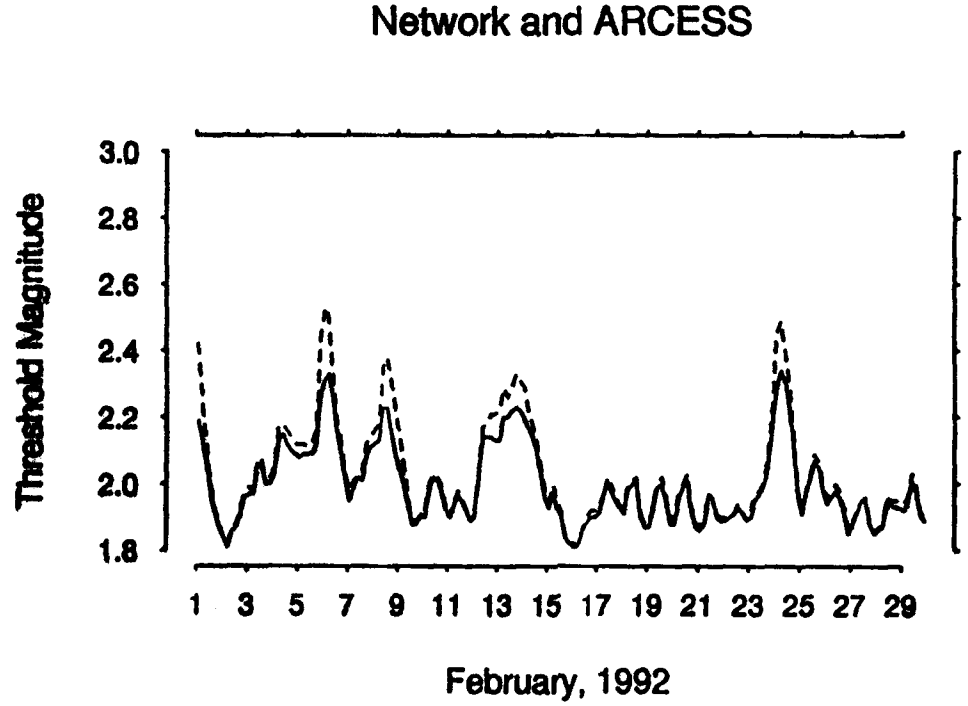

FIG. 4B. Four-hour medians of the magnitude thresholds for ARCESS and for the network for the month of February 1992.
Solid line: Network
Dashed line: ARCESS

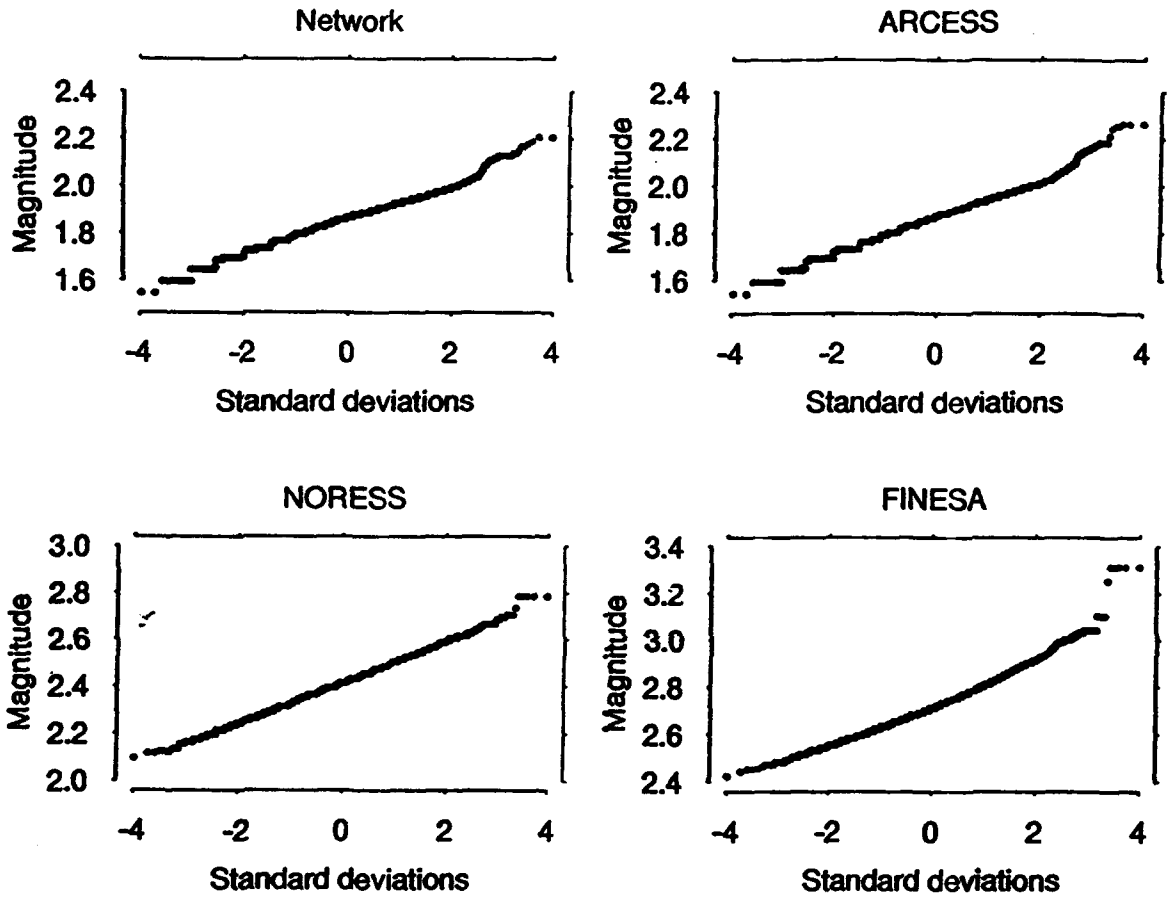

FIG. 5. Quantile plots of a nighttime interval without any strong events (February 27, 00:00 - 04:00).

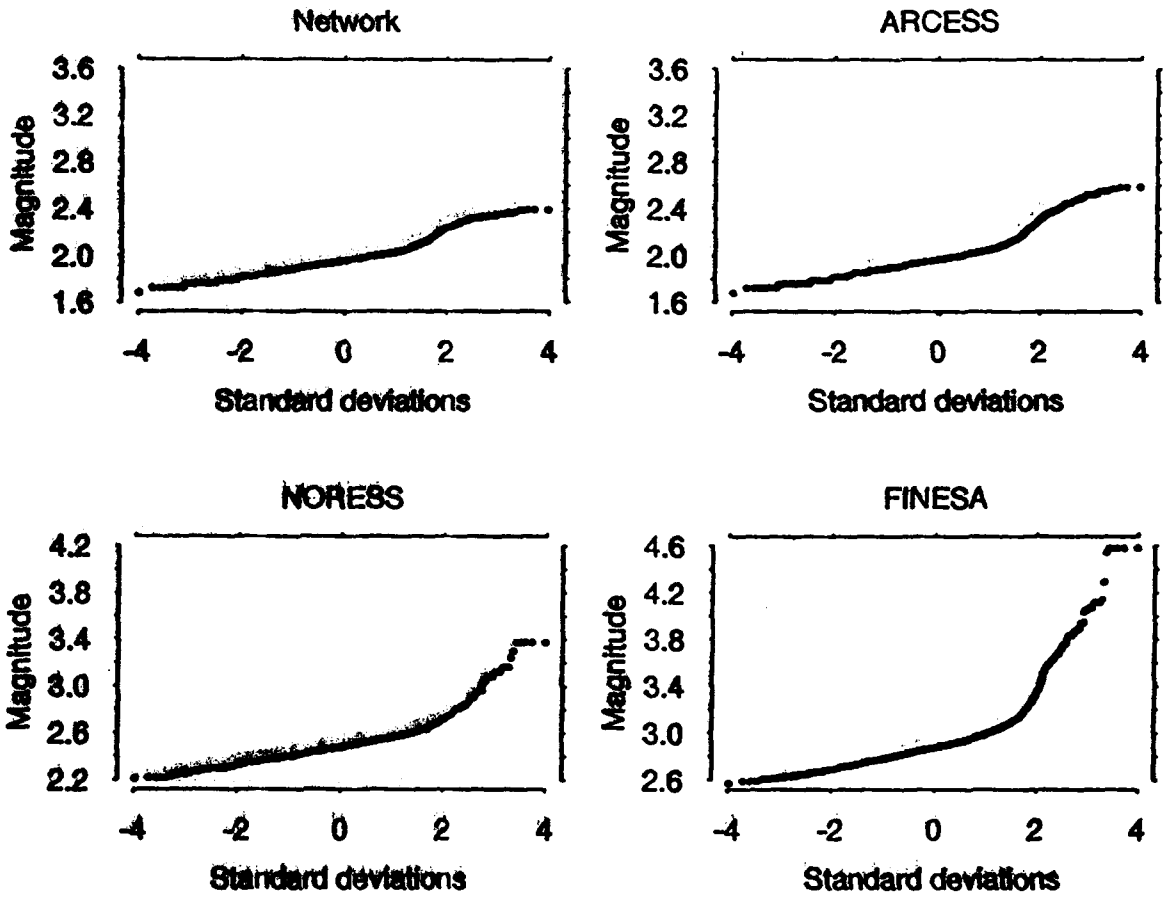

FIG. 6. Quantile plots of a daytime interval with many events (February 26, 10:00 - 14:00).

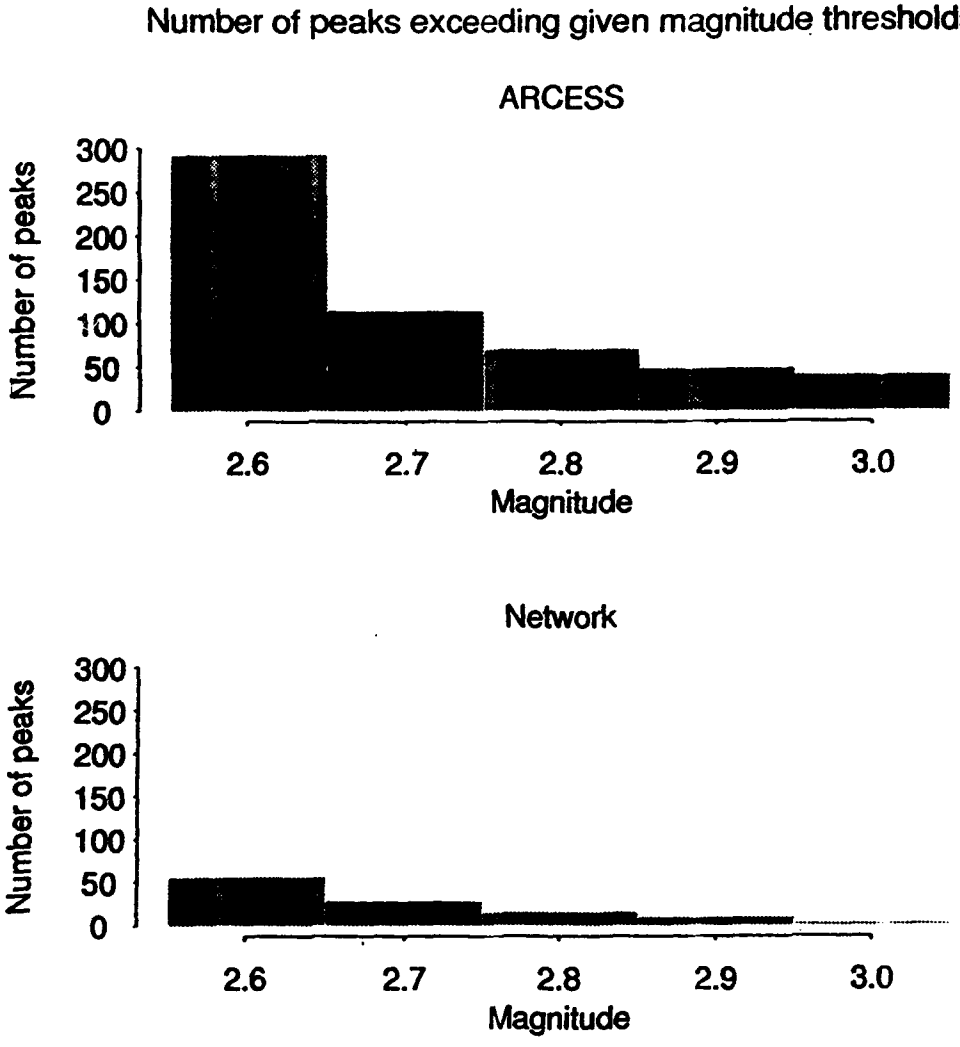

FIG. 7. Number of peaks exceeding given magnitude thresholds.
Upper part: ARCESS
Lower part: Network

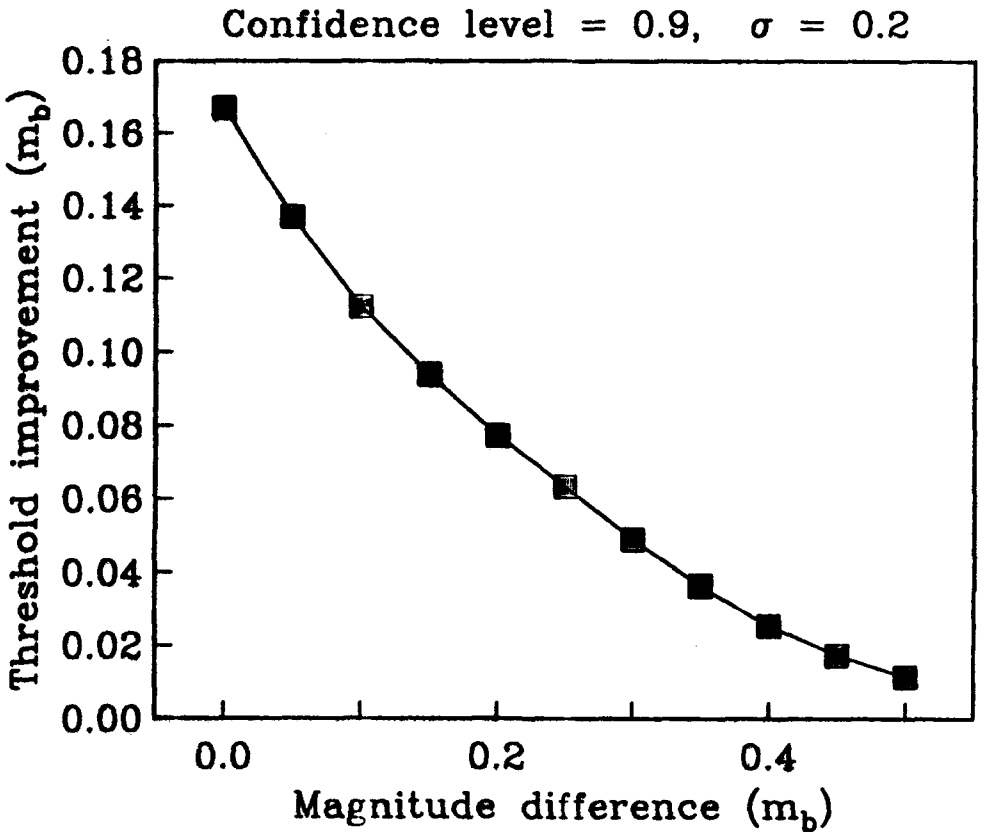

FIG. 8. Improvement of the combined 90% magnitude thresholds of two observations, as a function of the magnitude difference between them. The assumed standard deviation of the magnitude estimates are 0.2, which also was the value used for monitoring the northern Novaya Zemlya test site.

APPENDIX

This appendix contains figures A-1 through A-29, showing CSTM traces for each day of February 1992. The upper three traces of each figure represent the magnitude thresholds obtained from the three individual arrays, whereas the bottom trace illustrates the network threshold.

The arrow indicate peaks with network magnitude threshold exceeding $m_b = 2.6$. A few peaks with slightly lower thresholds are also marked. A T at the arrow indicates that the peak is caused by signals from a teleseismic event, whereas an R indicates signals from a local or regional event. Peaks caused by a gap in the ARCESS recordings are marked by a G.

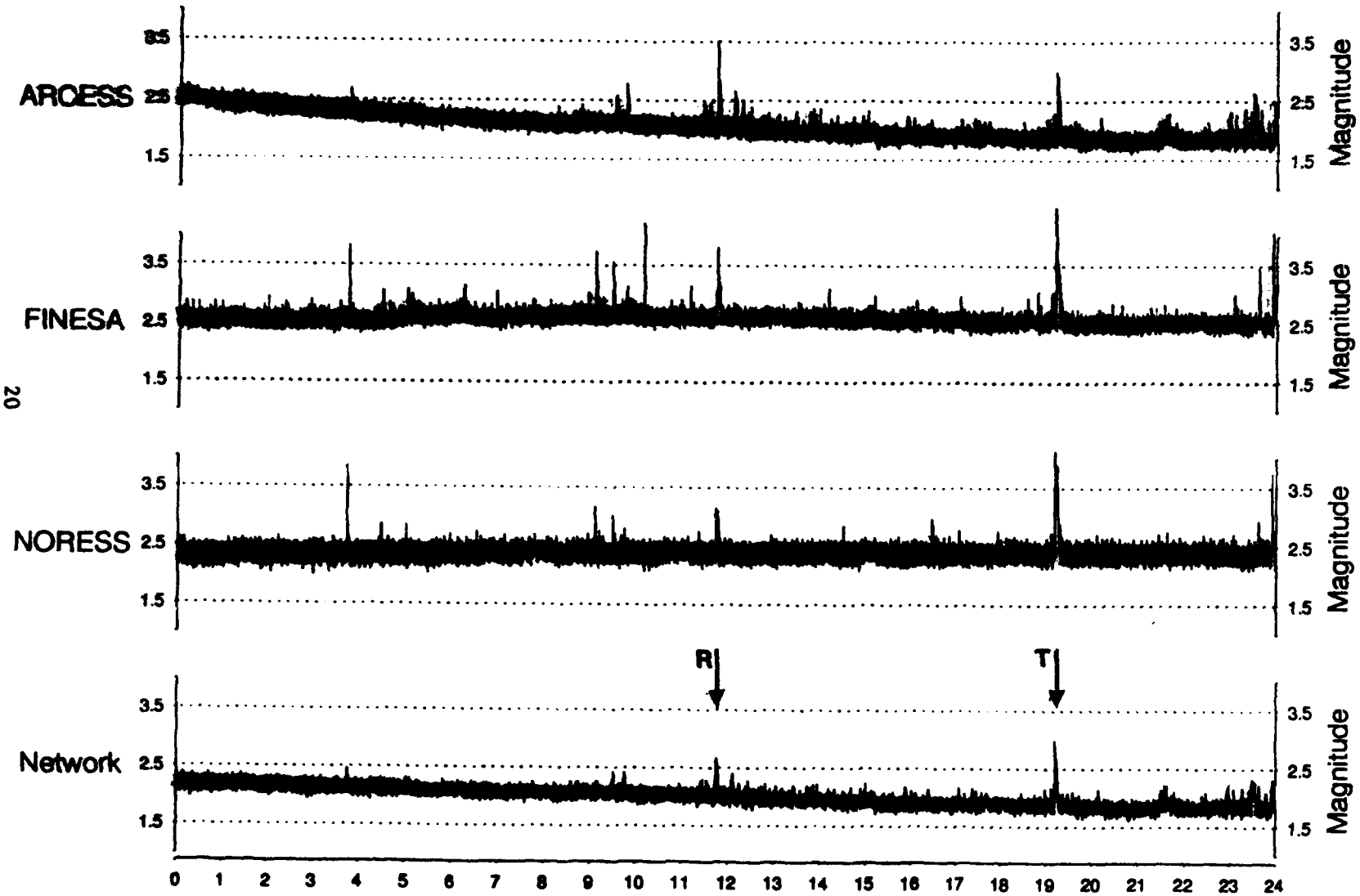
ARCESS
FINESA
NORESS
Network
3.5
2.5
1.5
Magnitude
R
T
0 1 2 3 4 5 6 7 8 9 10 11 12 13 14 15 16 17 18 19 20 21 22 23 24
Hours (GMT)
February 1, 1992

FIGURE A-1

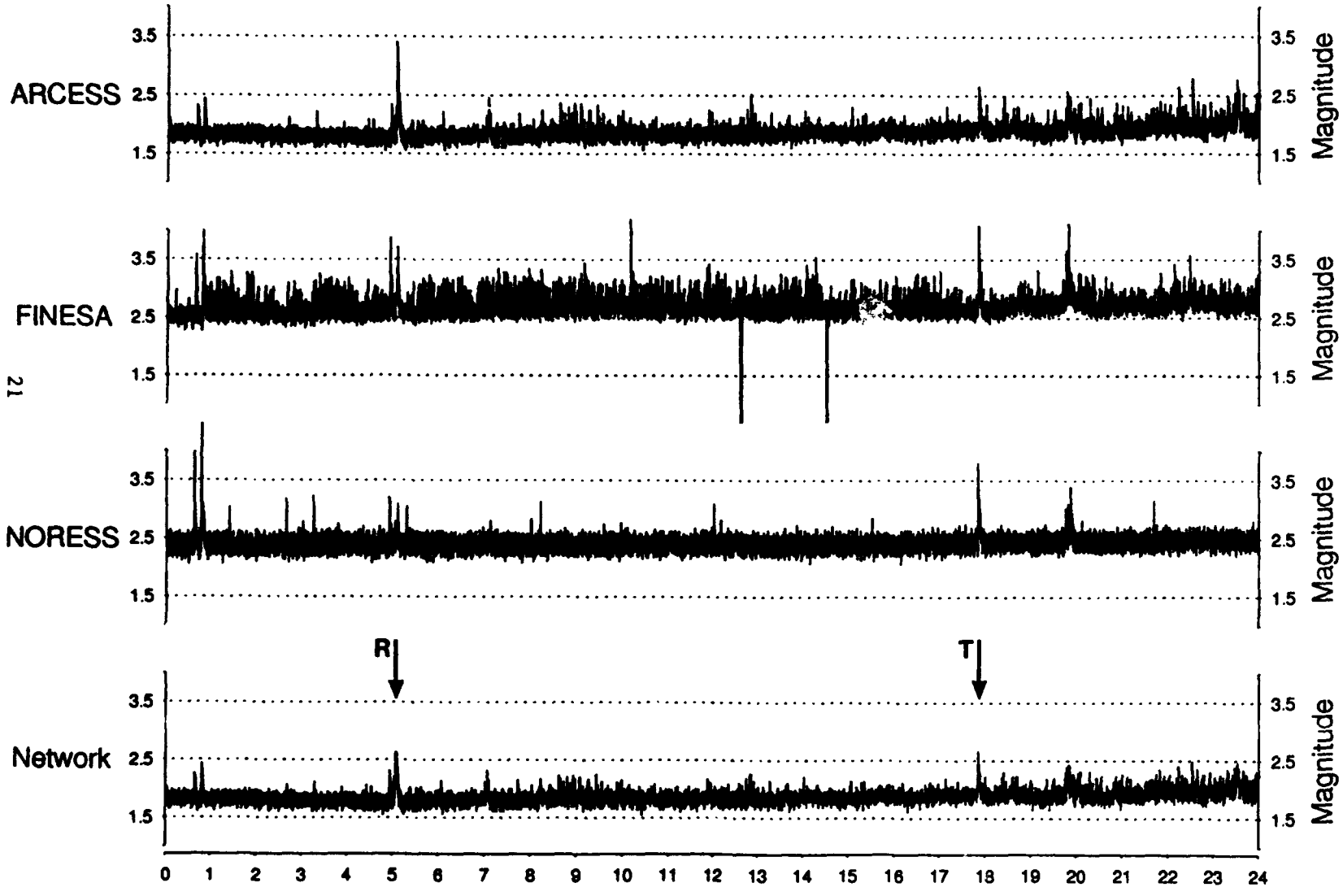

February 2, 1992

FIGURE A-2

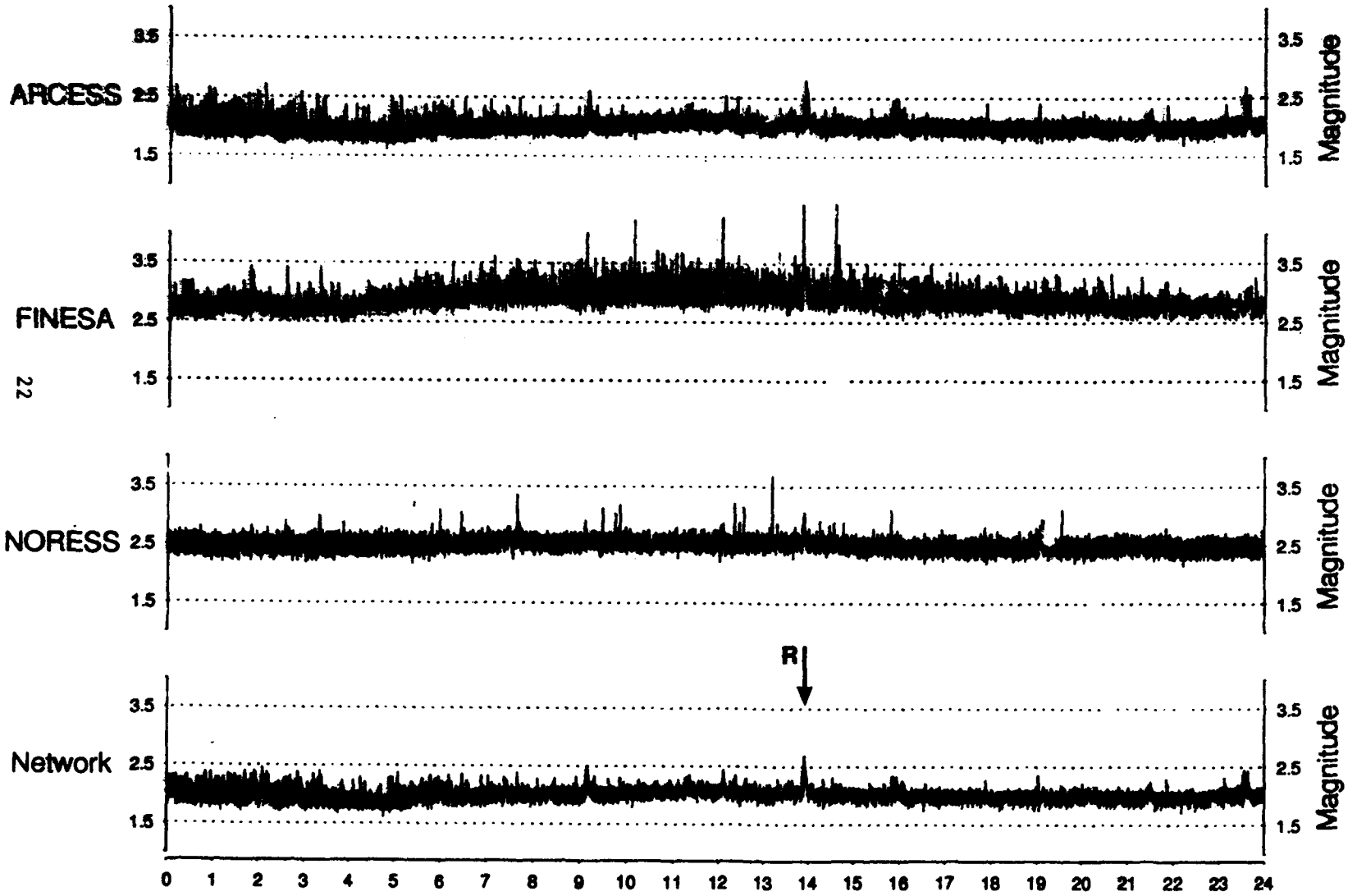

February 3, 1992

FIGURE A-3

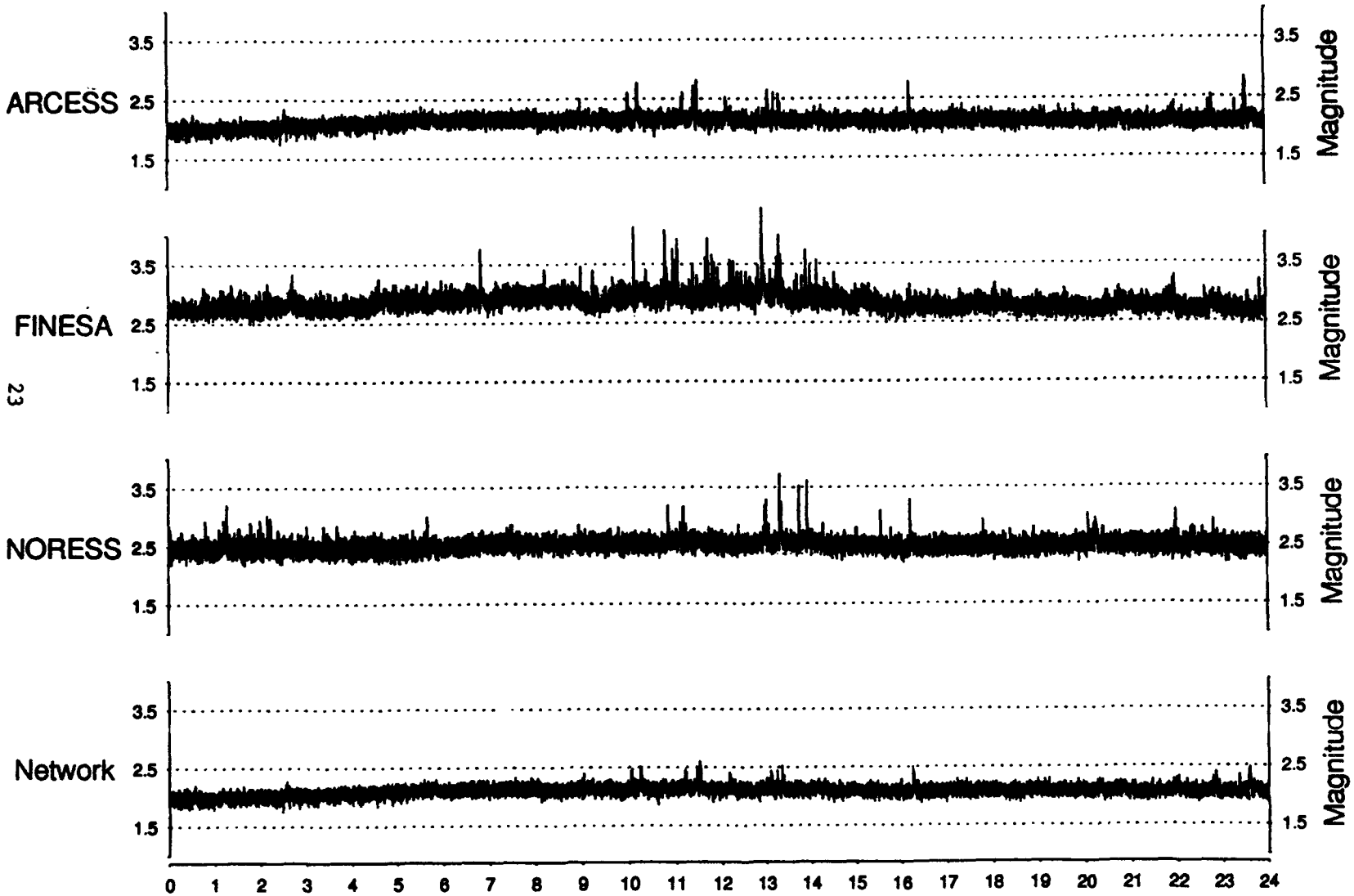

February 4, 1992

FIGURE A-4

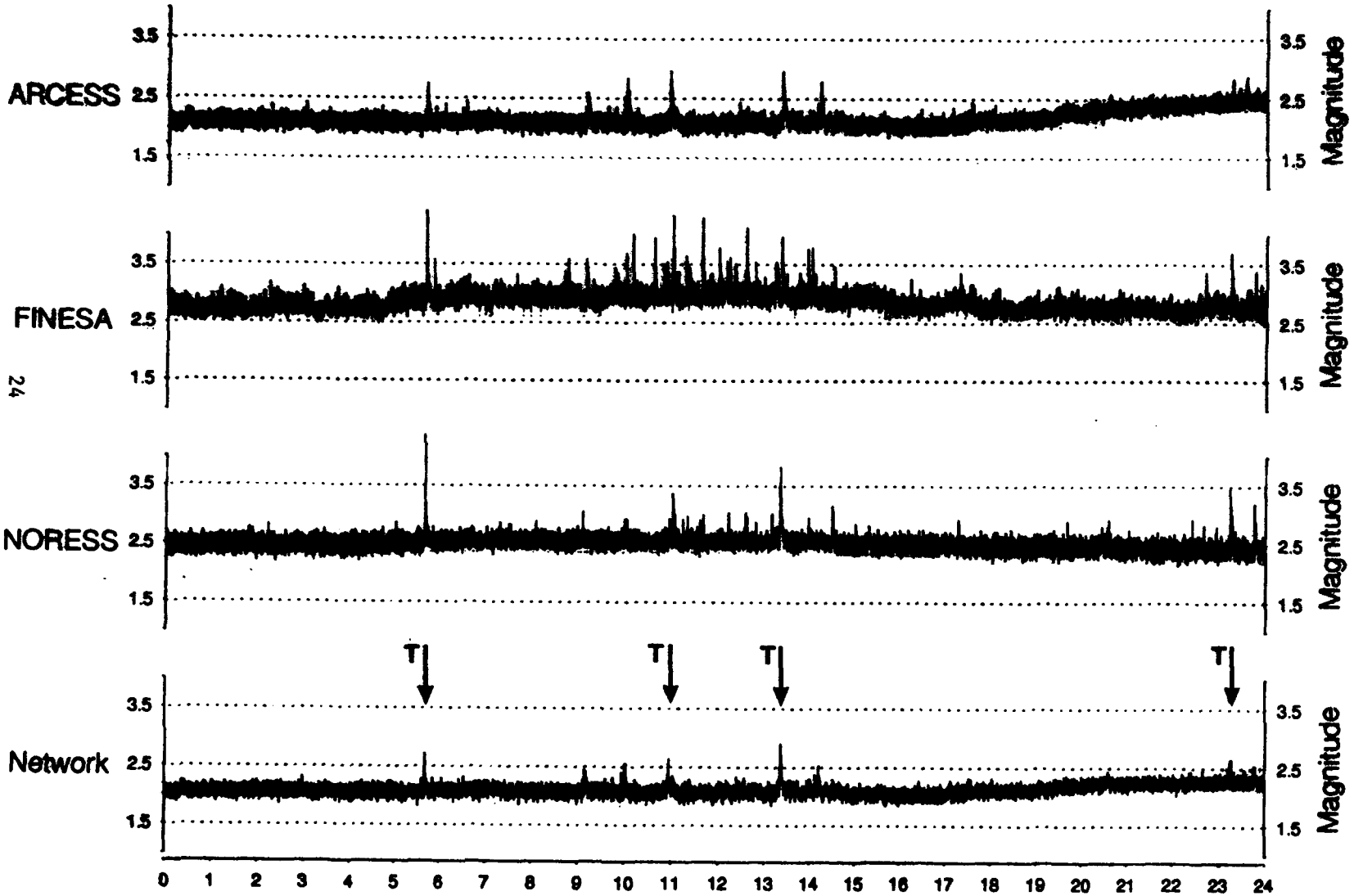

February 5, 1992

FIGURE A-5

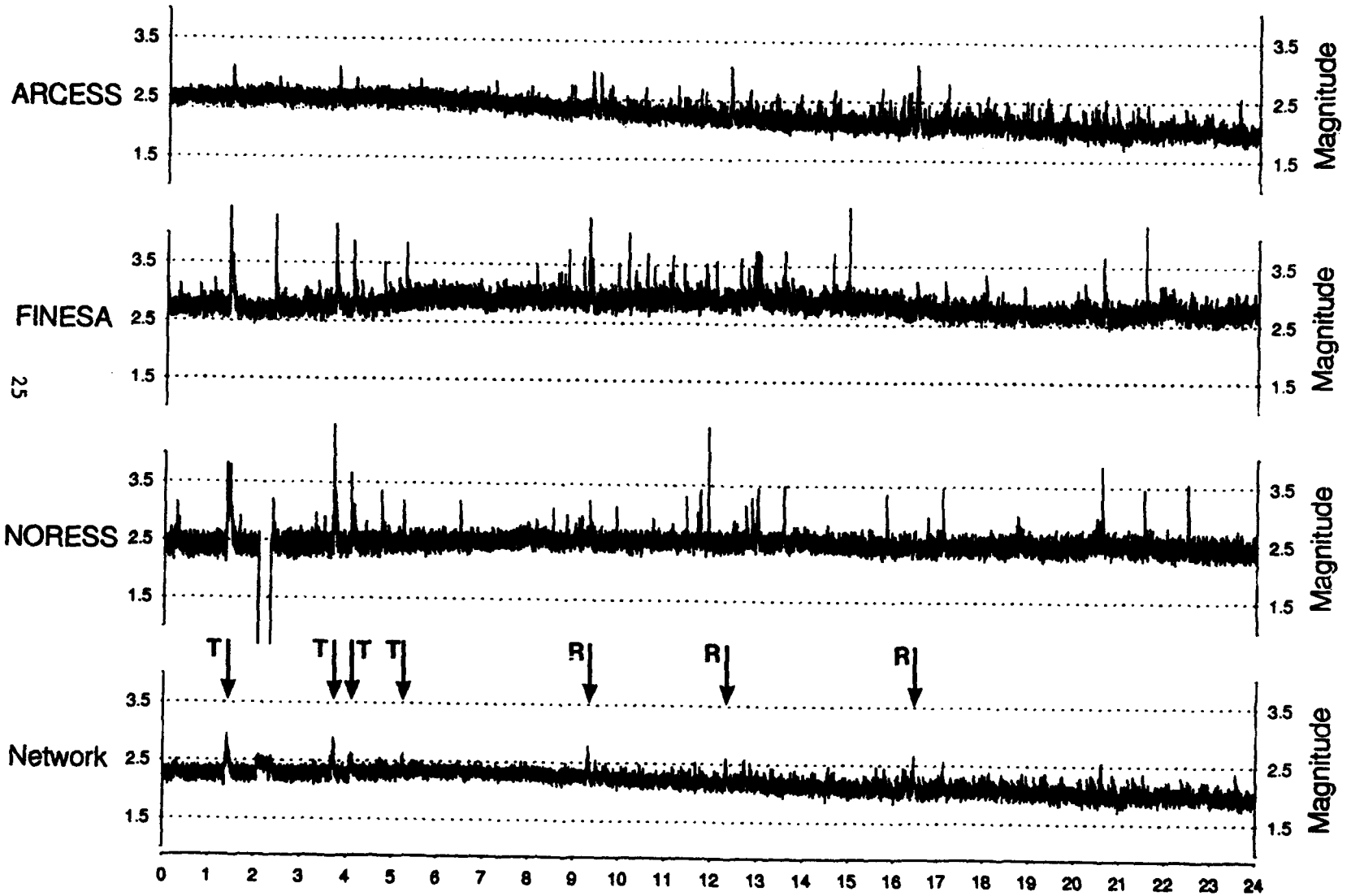

February 6, 1992

FIGURE A-6

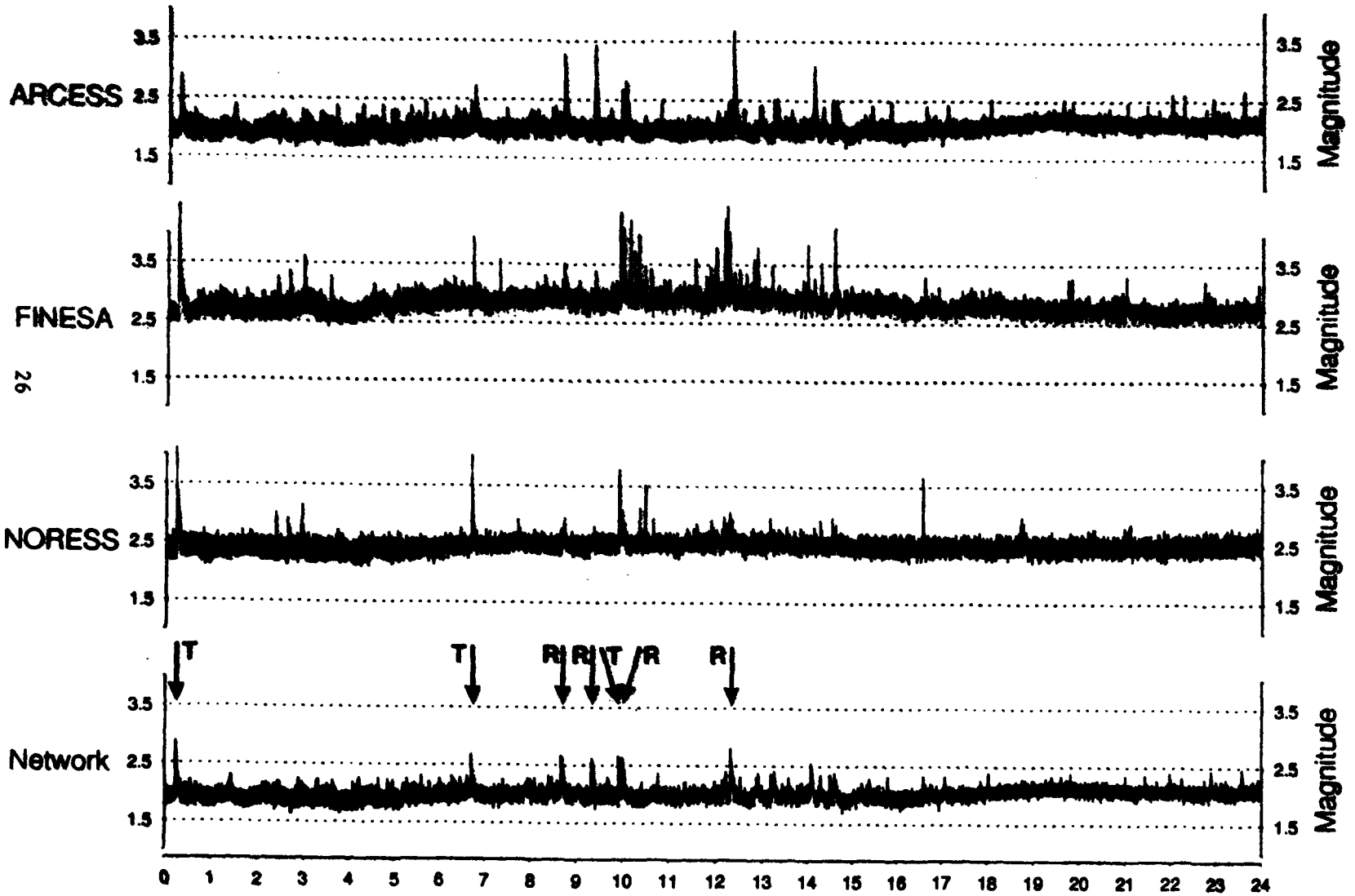

February 7, 1992

FIGURE A-7

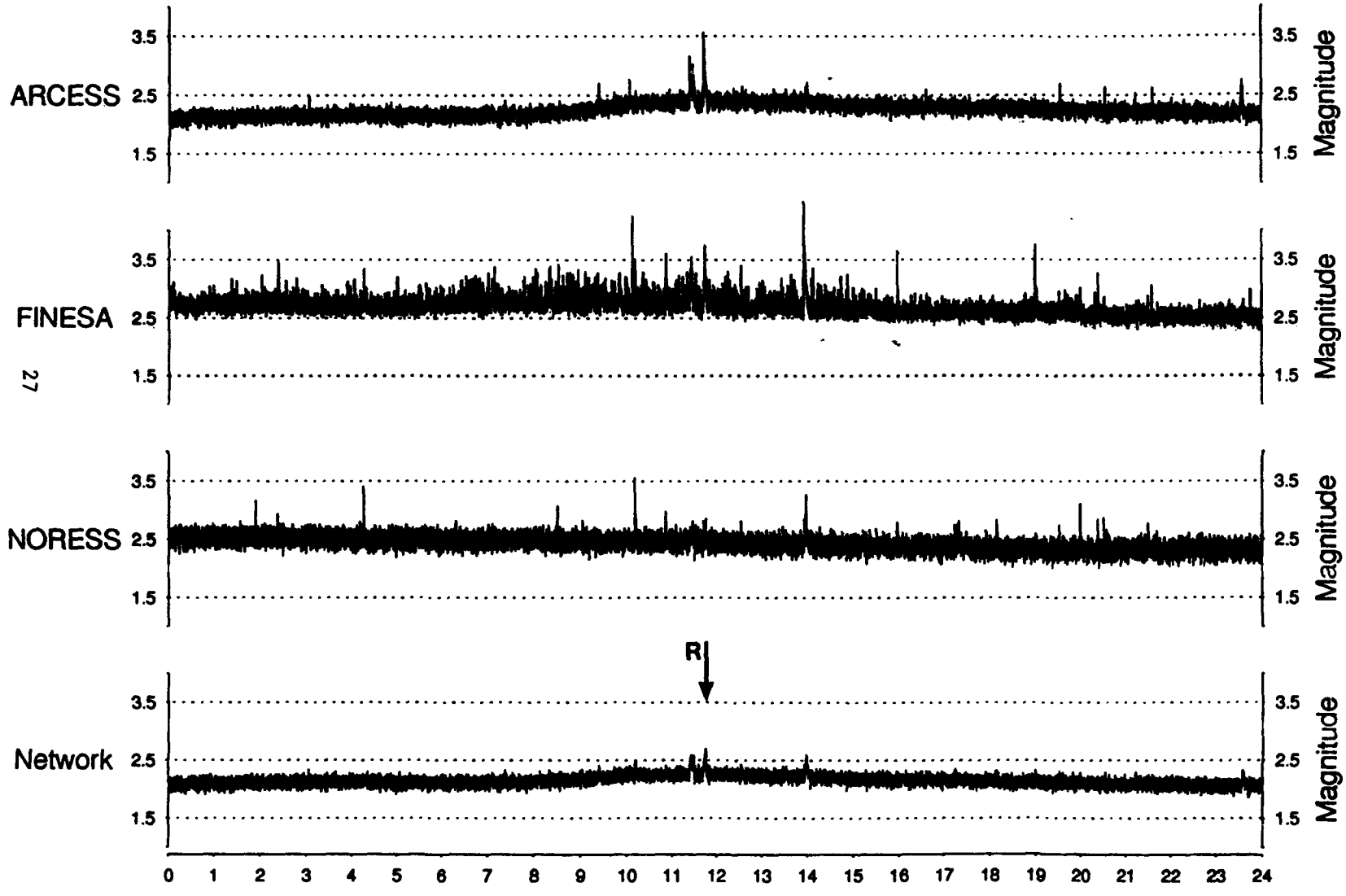

February 8, 1992

FIGURE A-8

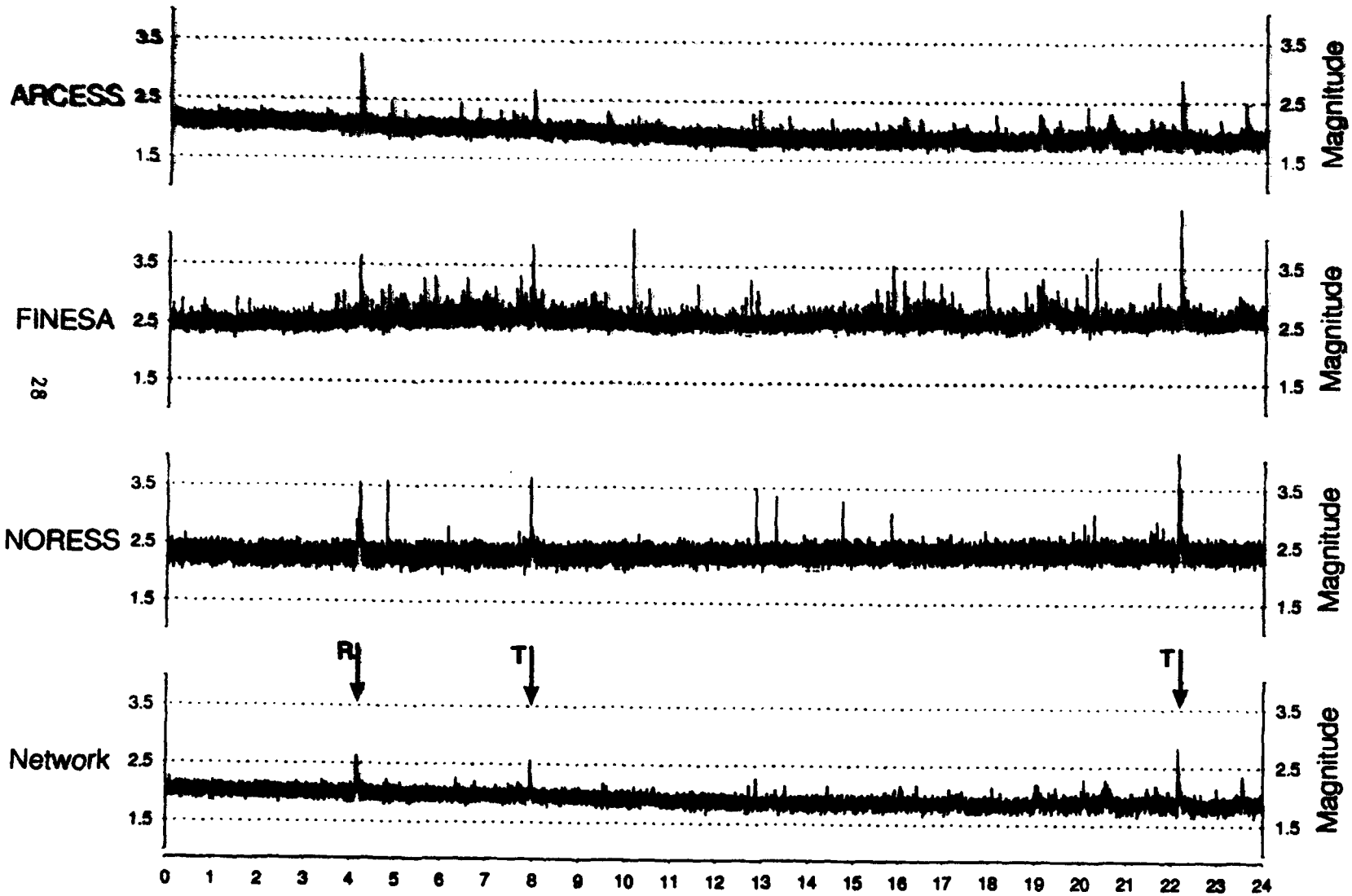

February 9, 1992

FIGURE A-9

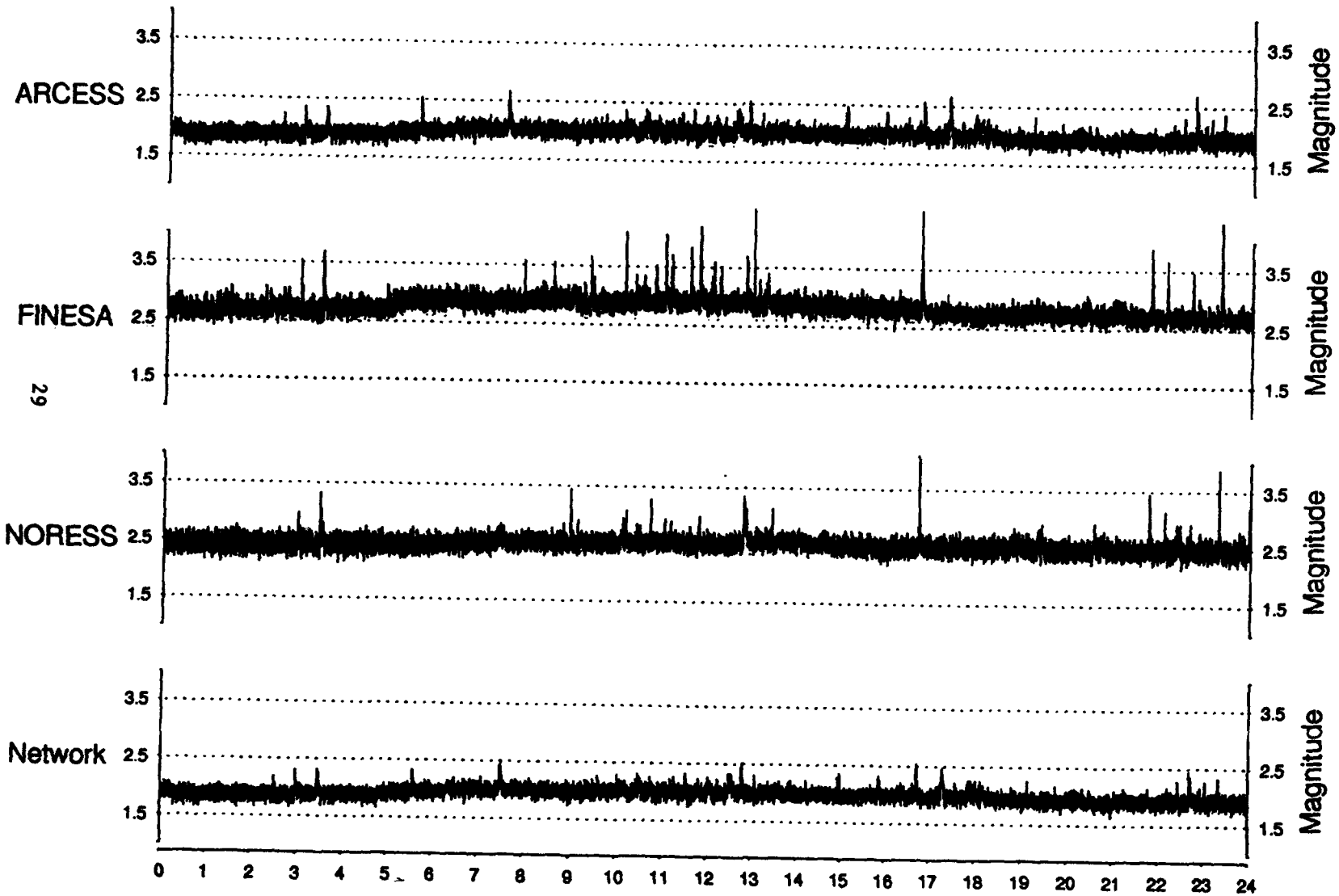

February 10, 1992

FIGURE A-10

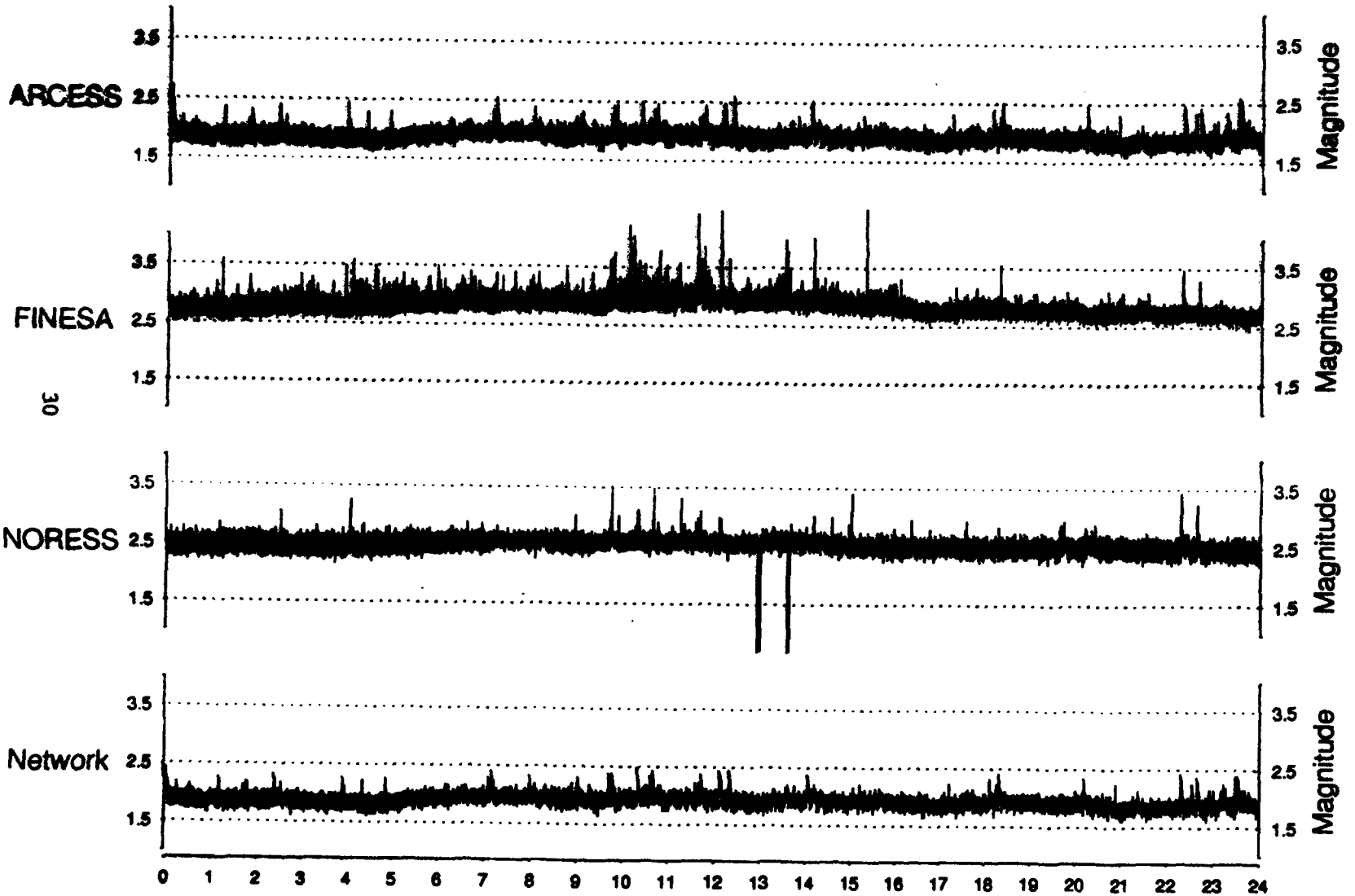

30

February 11, 1992

FIGURE A-11

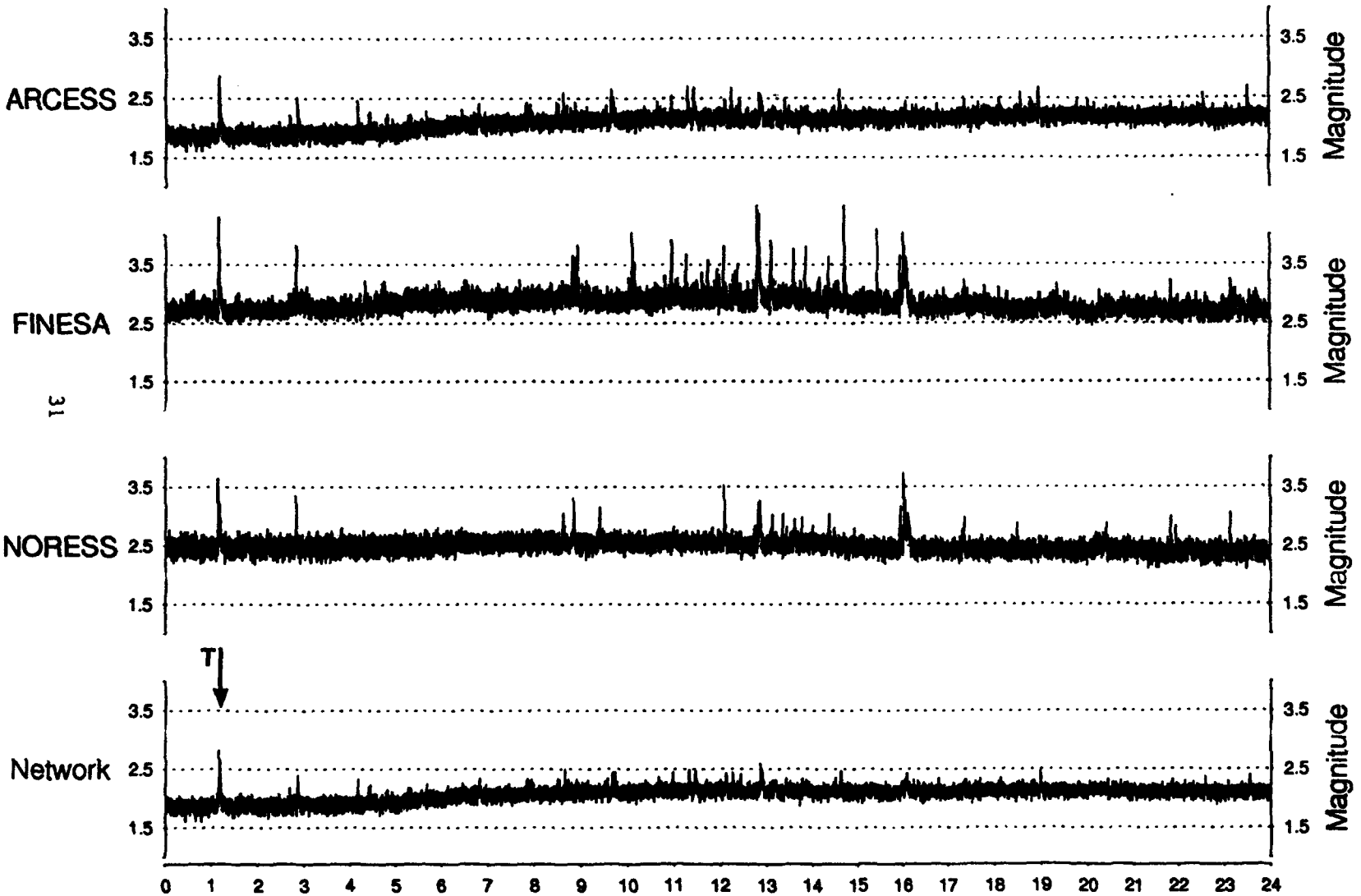

February 12, 1992

FIGURE A-12

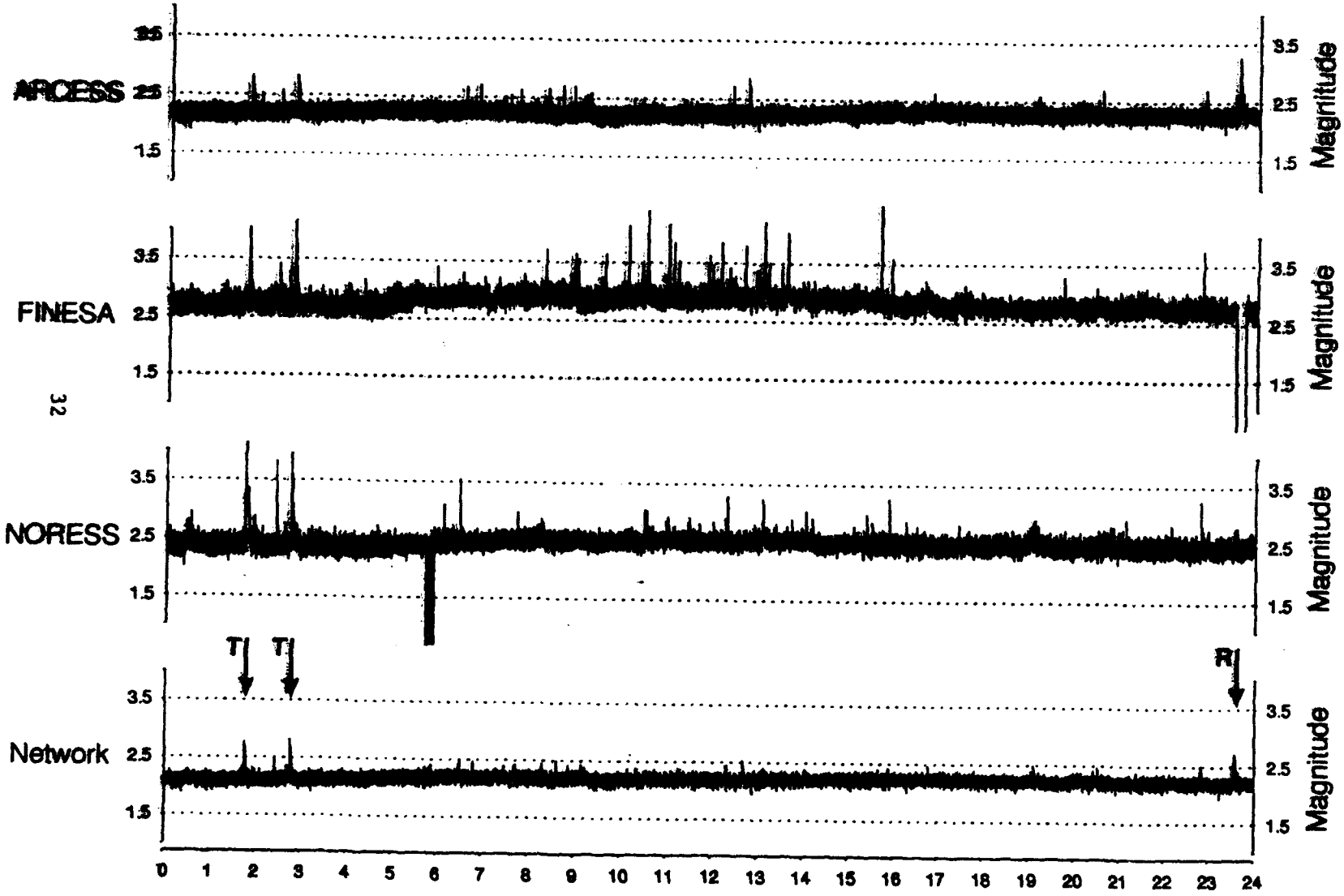

February 13, 1992

FIGURE A-13

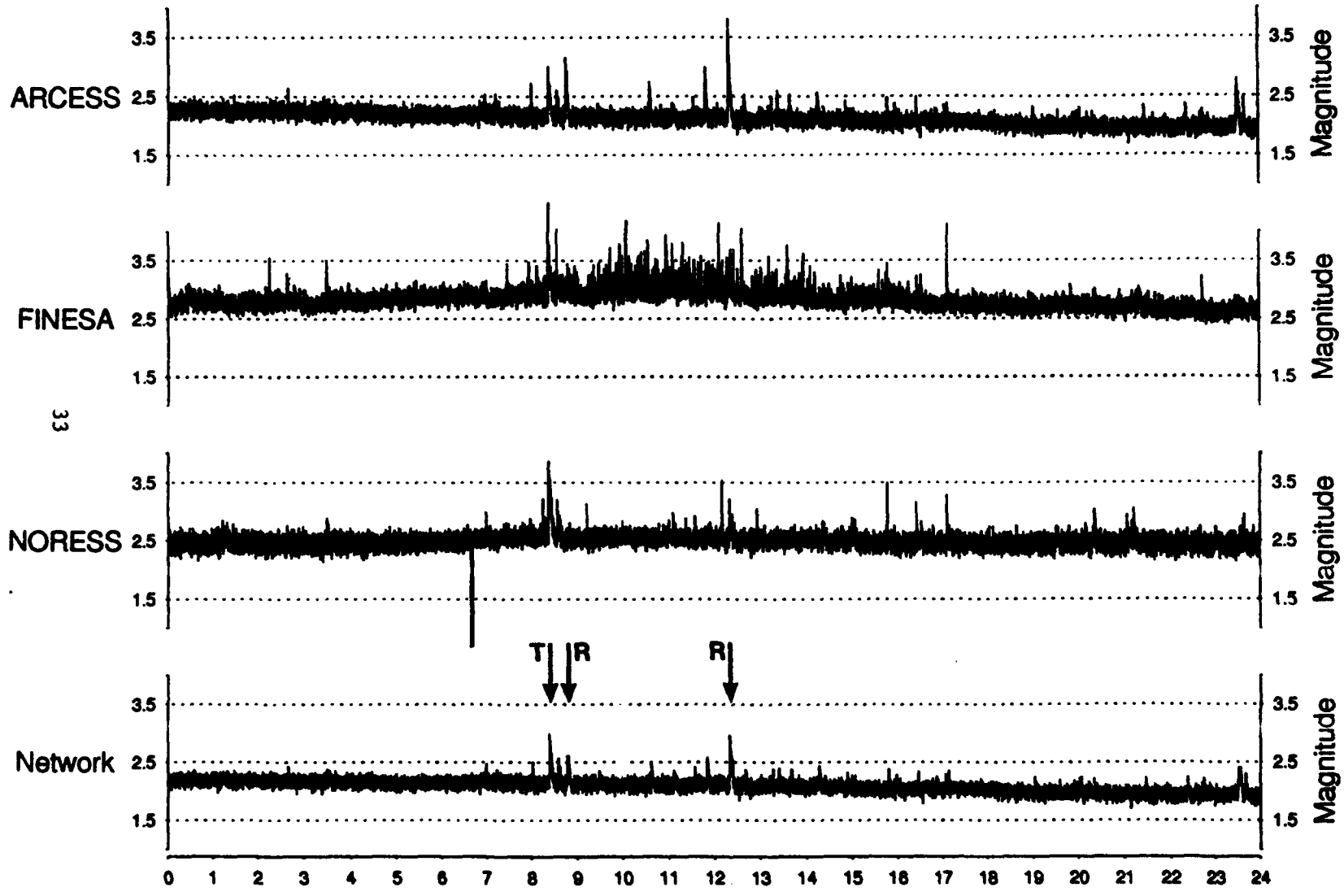

February 14, 1992

FIGURE A-14

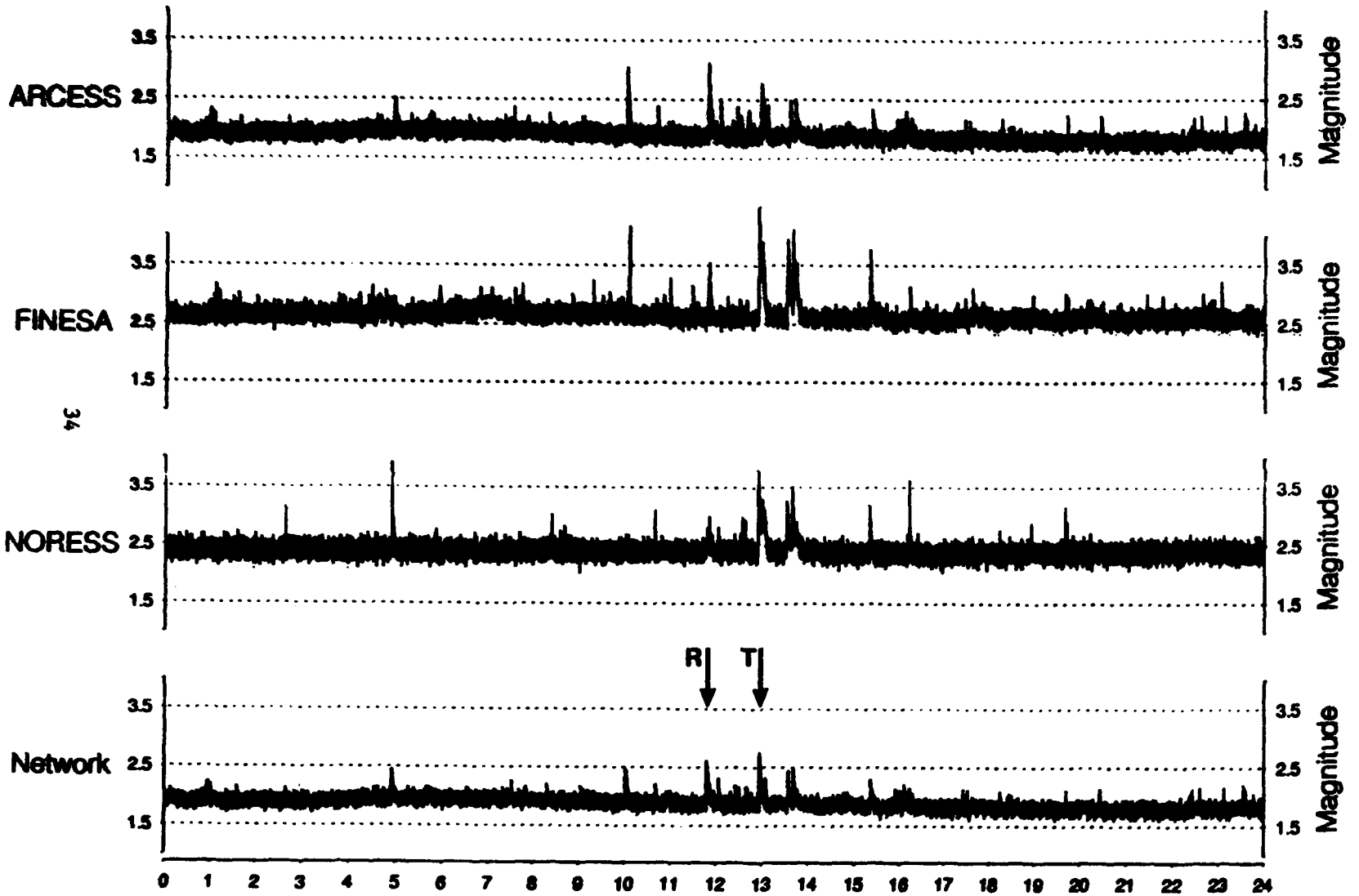

February 15, 1992

FIGURE A-15

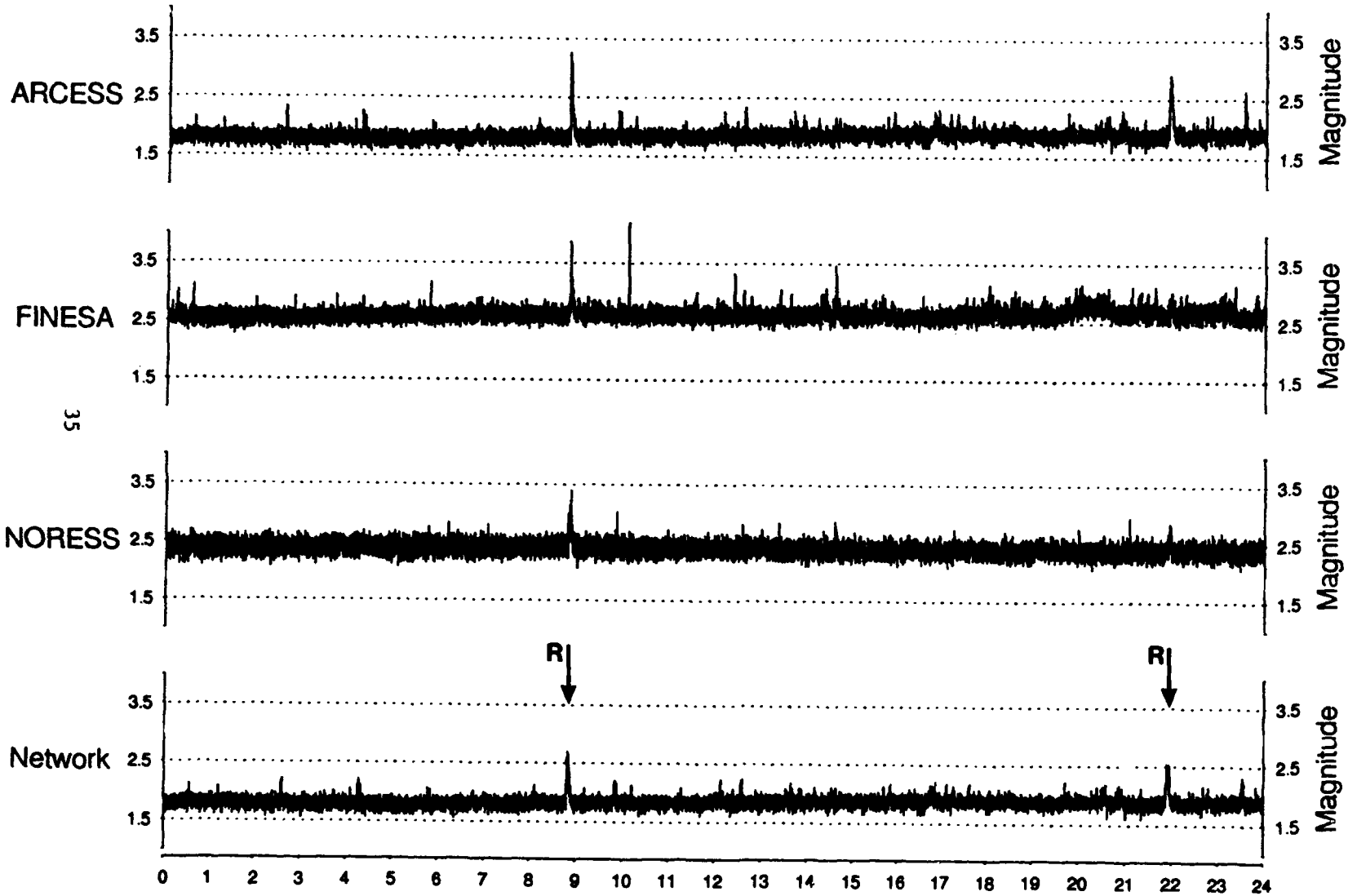

February 16, 1992

FIGURE A-16

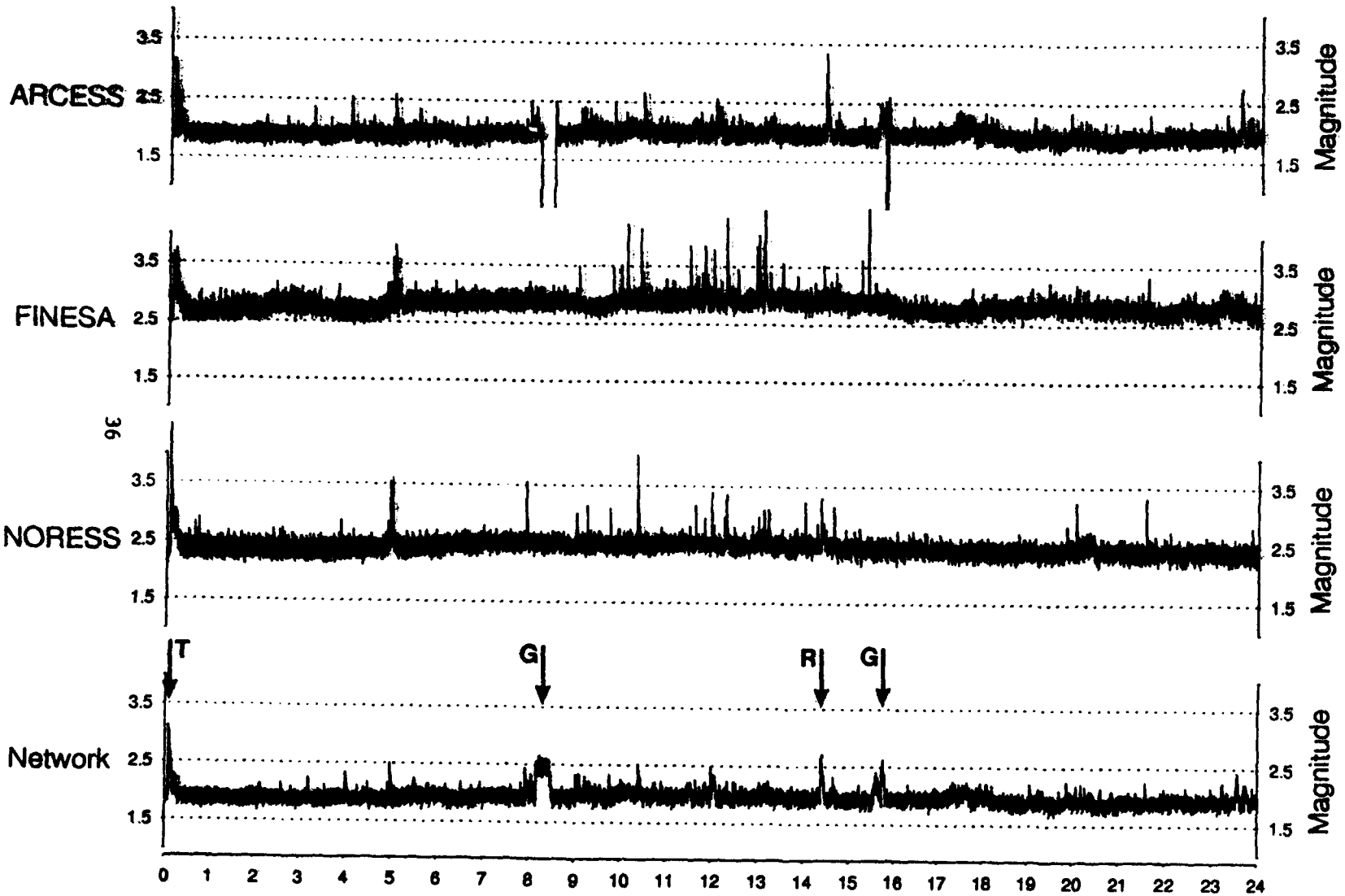

February 17, 1992

FIGURE A-17

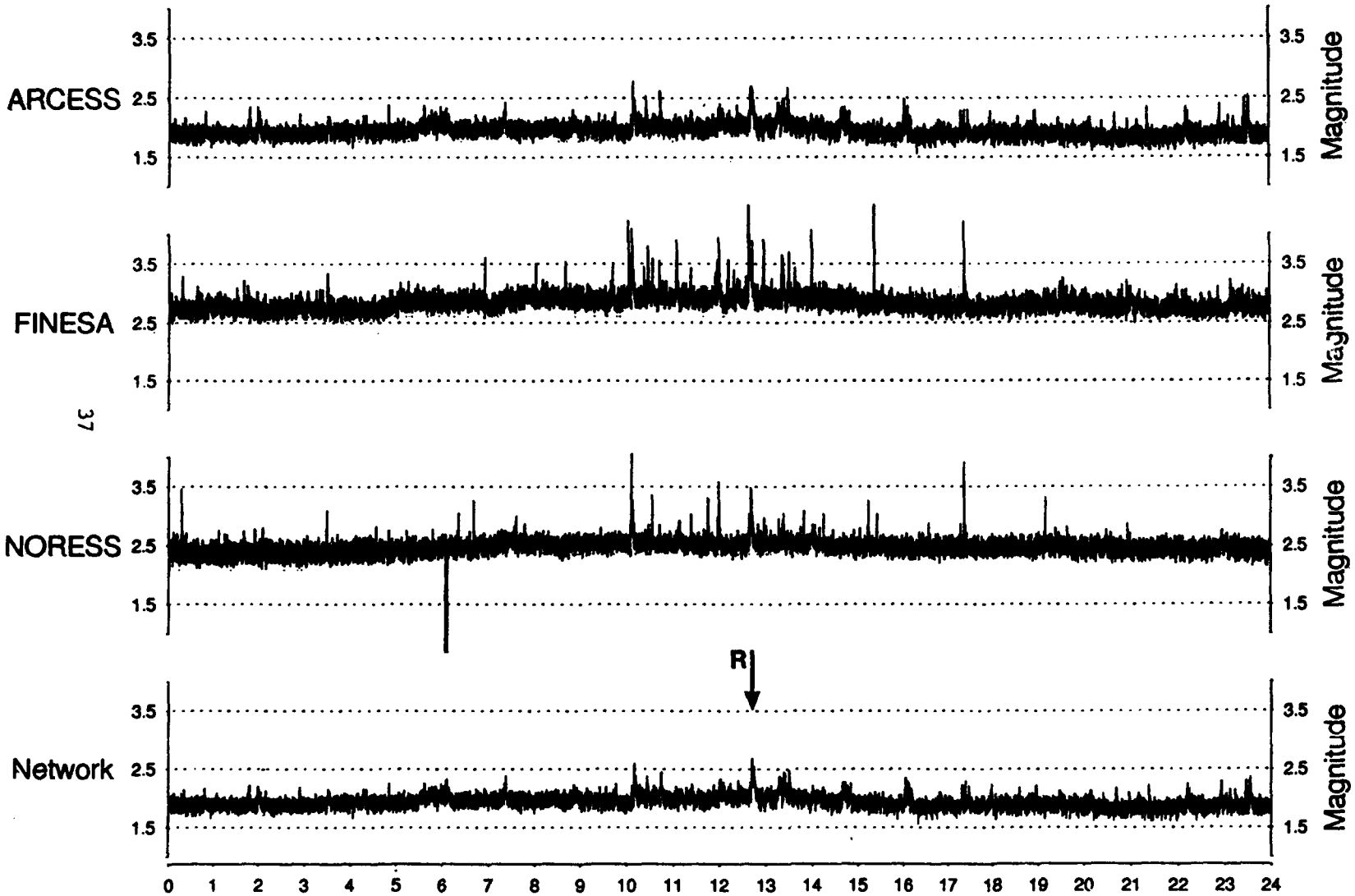

February 18, 1992

FIGURE A-18

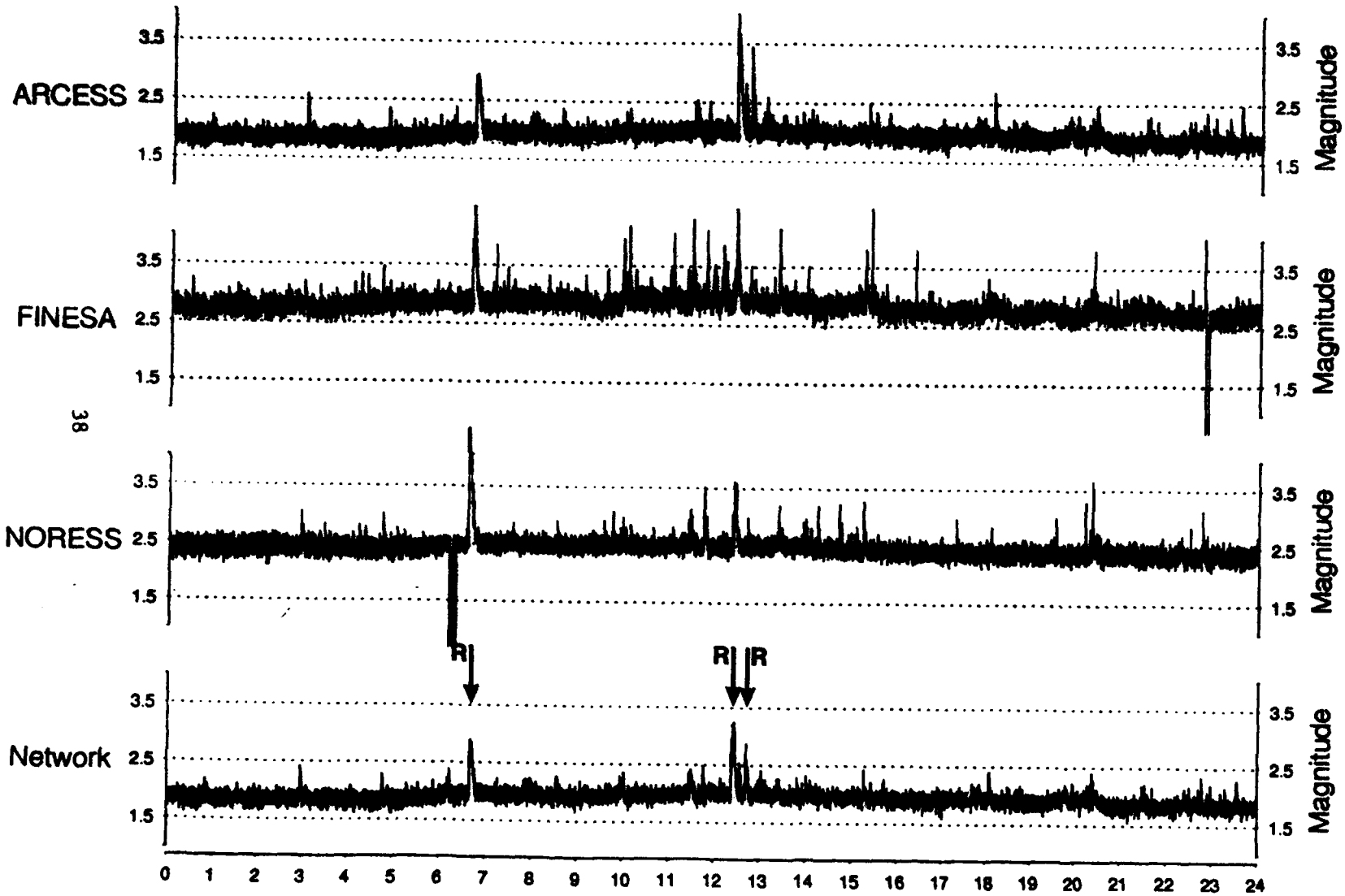

February 19, 1992

FIGURE A-19

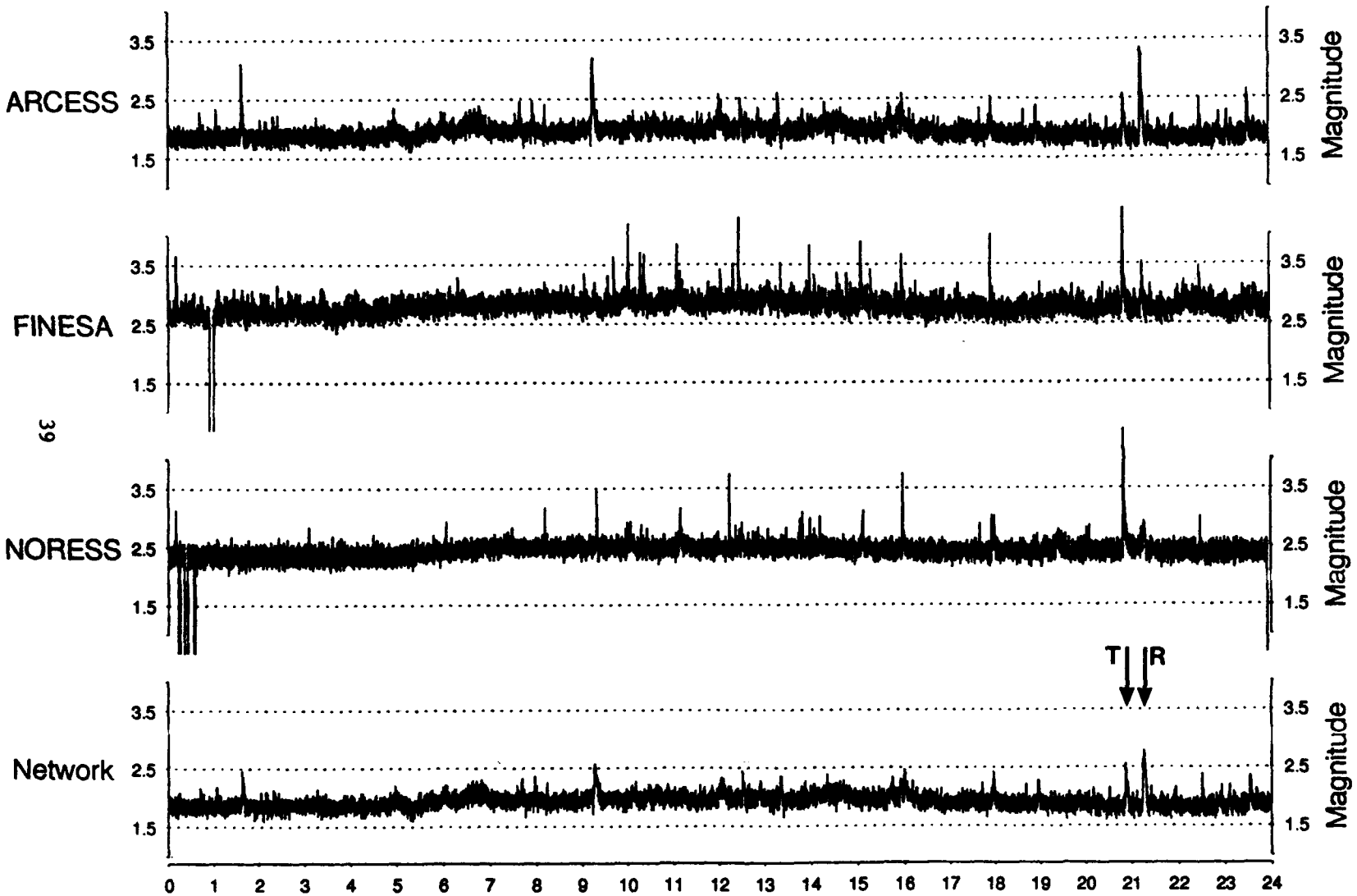

February 20, 1992

FIGURE A-20

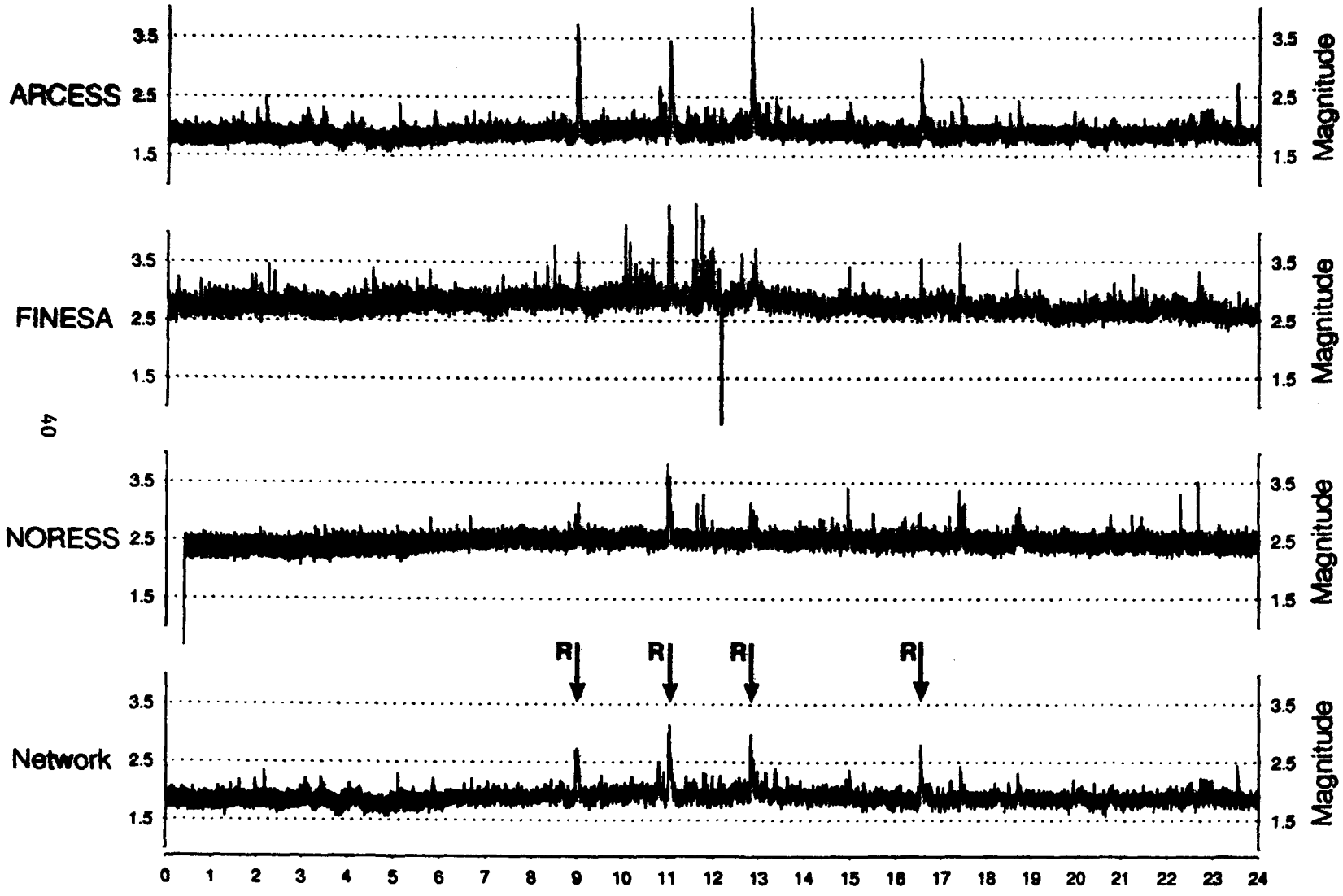

February 21, 1992

FIGURE A-21

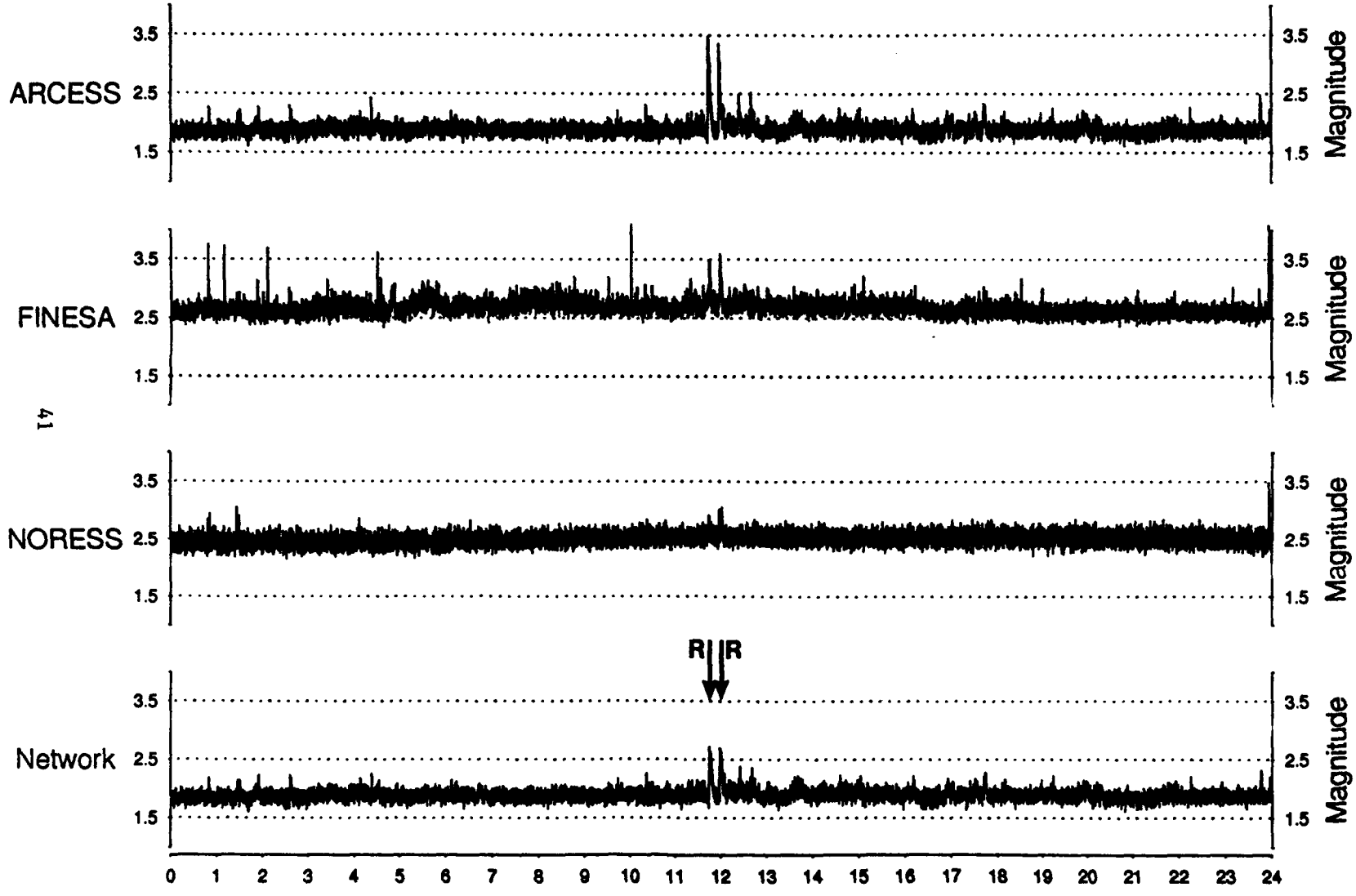

February 22, 1992

FIGURE A-22

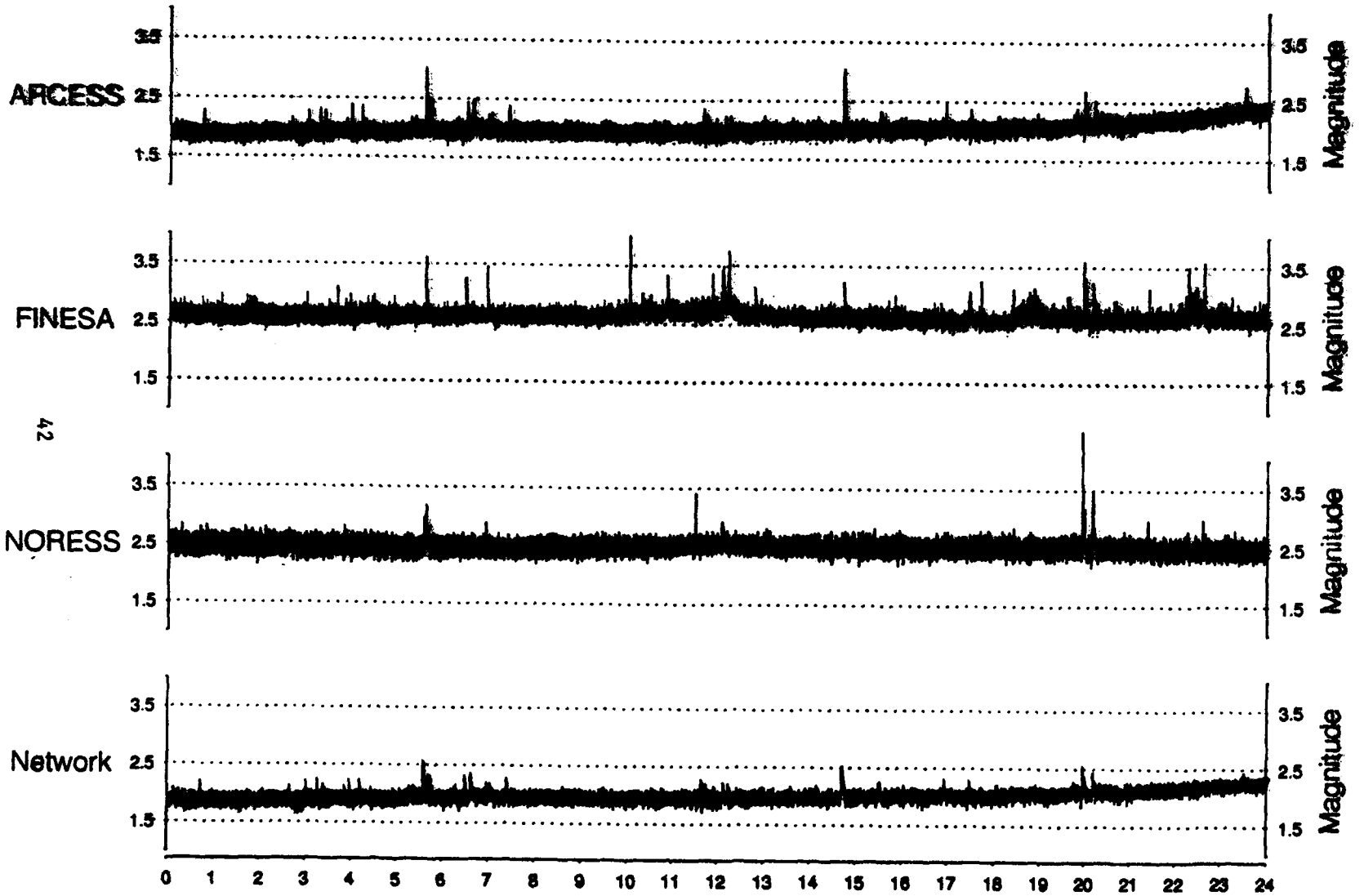

February 23, 1992

FIGURE A-23

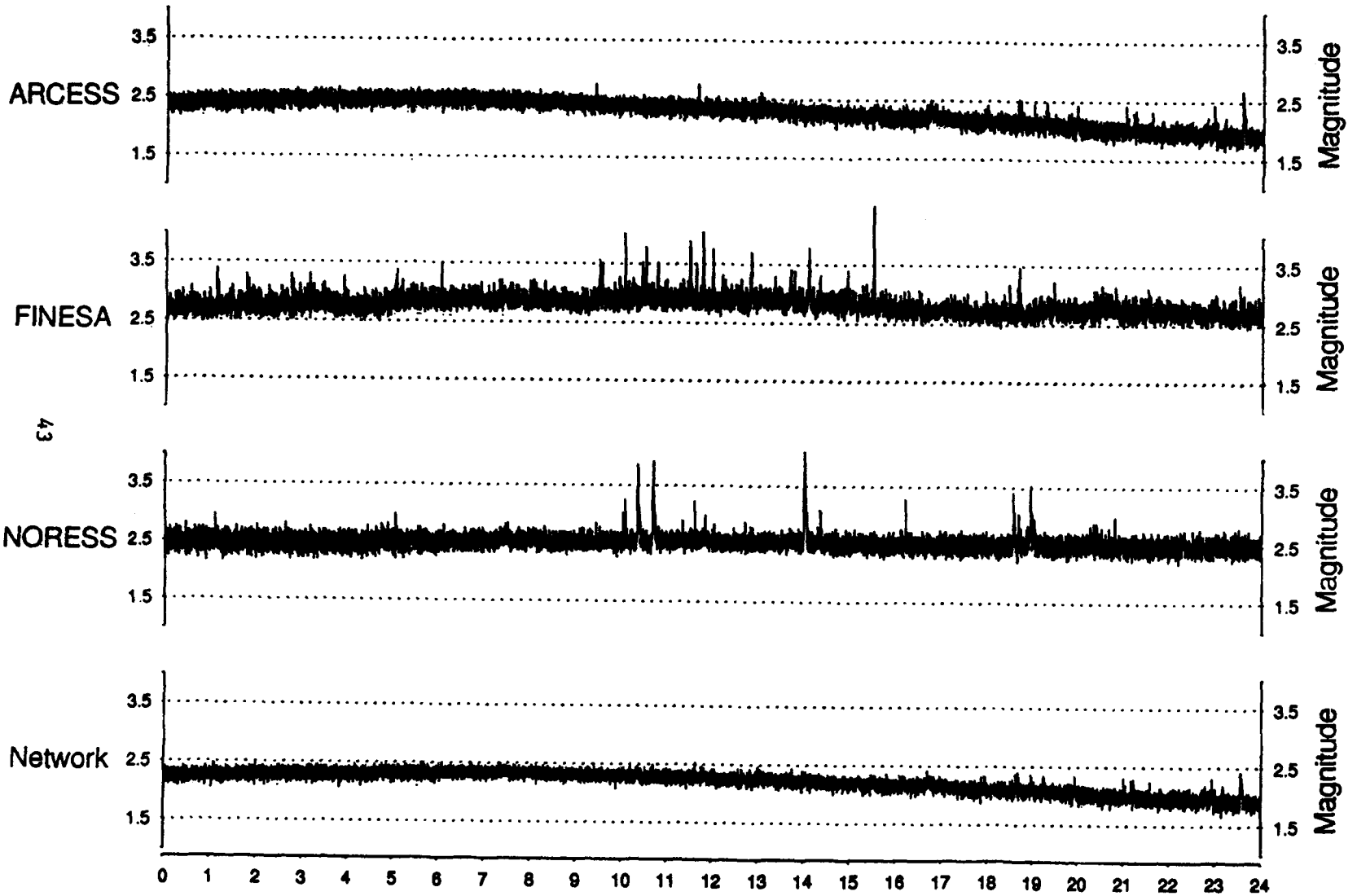

February 24, 1992

FIGURE A-24

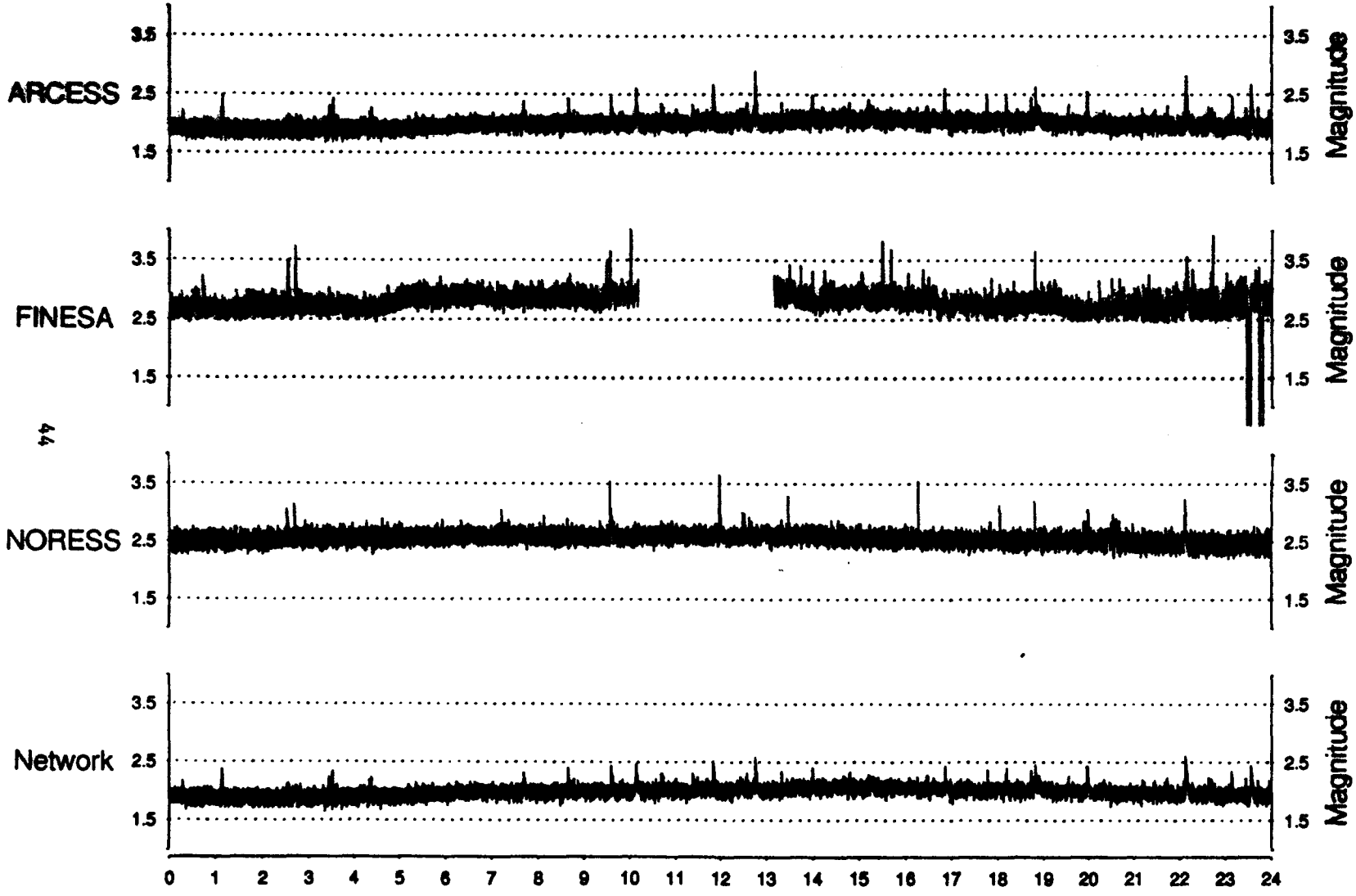

February 25, 1992

FIGURE A-25

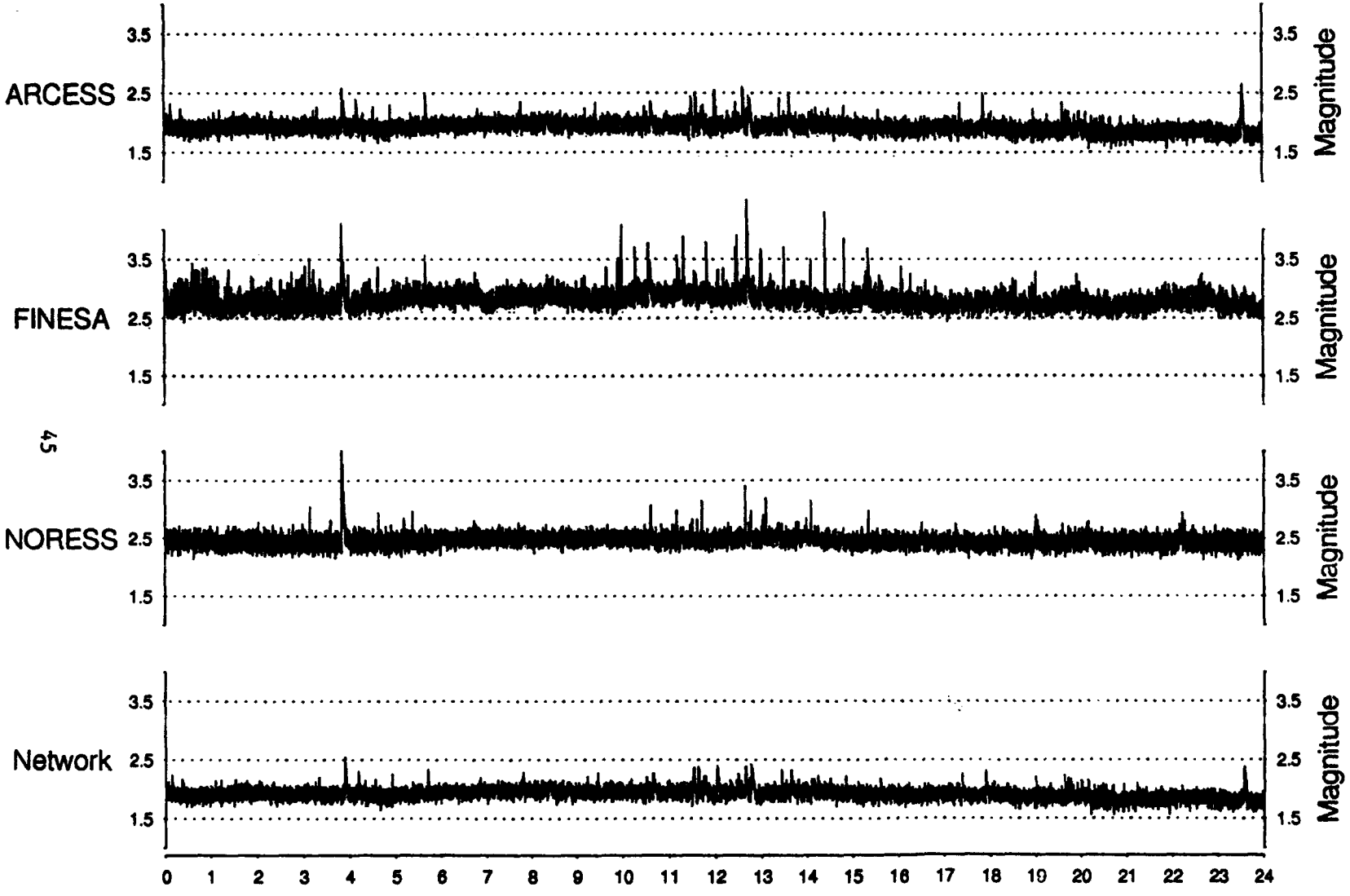

February 26, 1992

FIGURE A-26

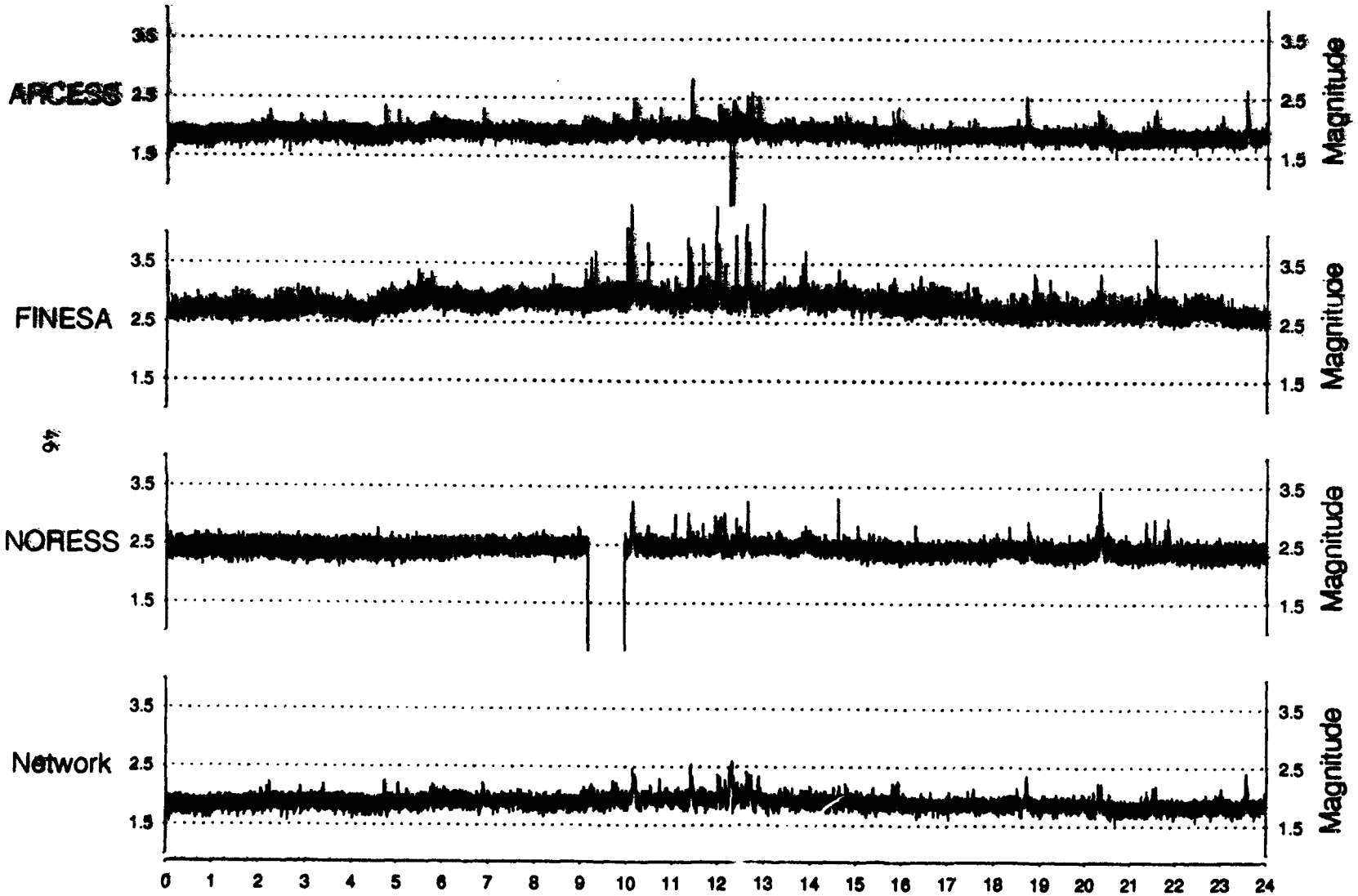

February 27, 1992

FIGURE A-27

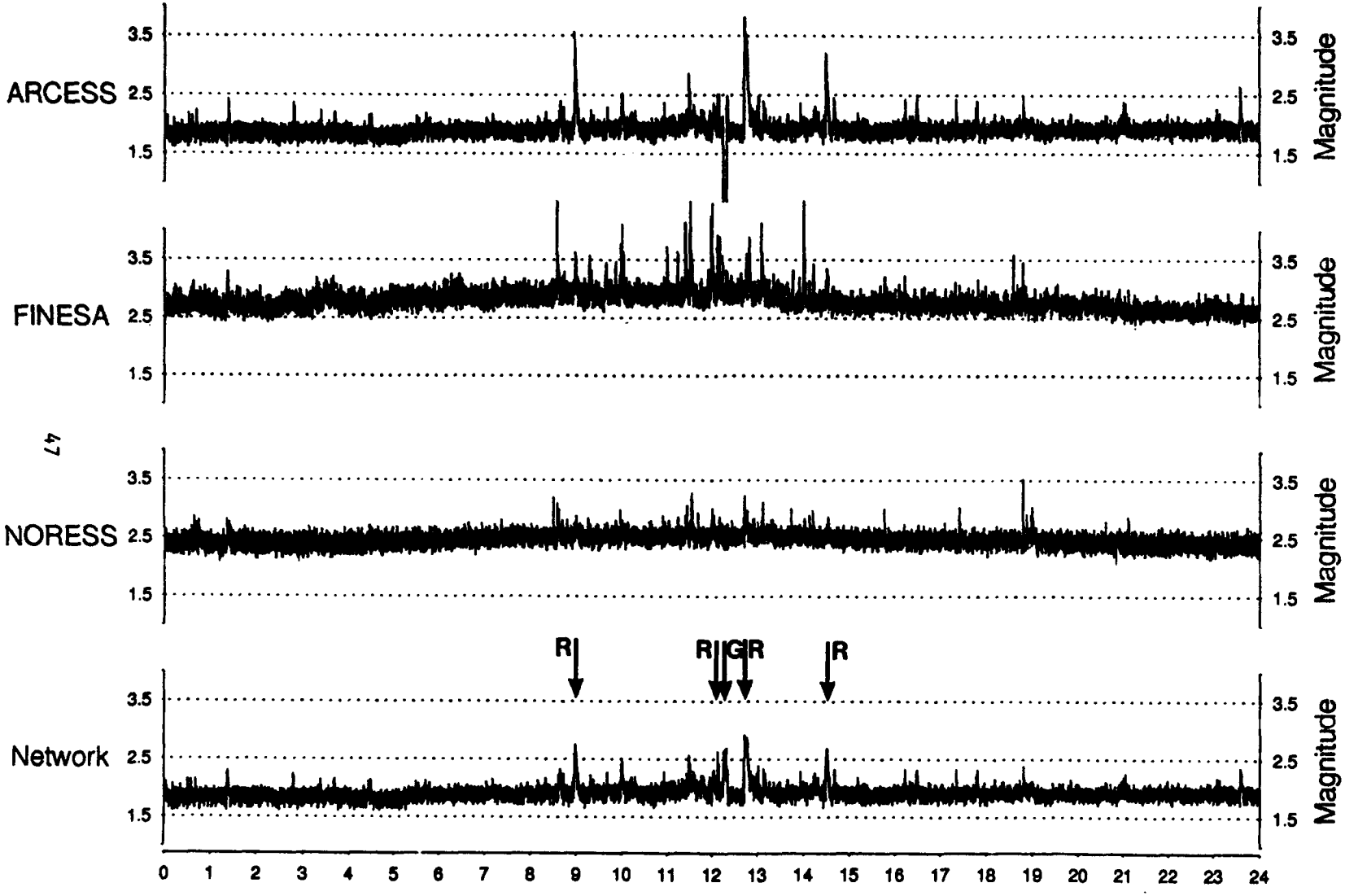

February 28, 1992

FIGURE A-28

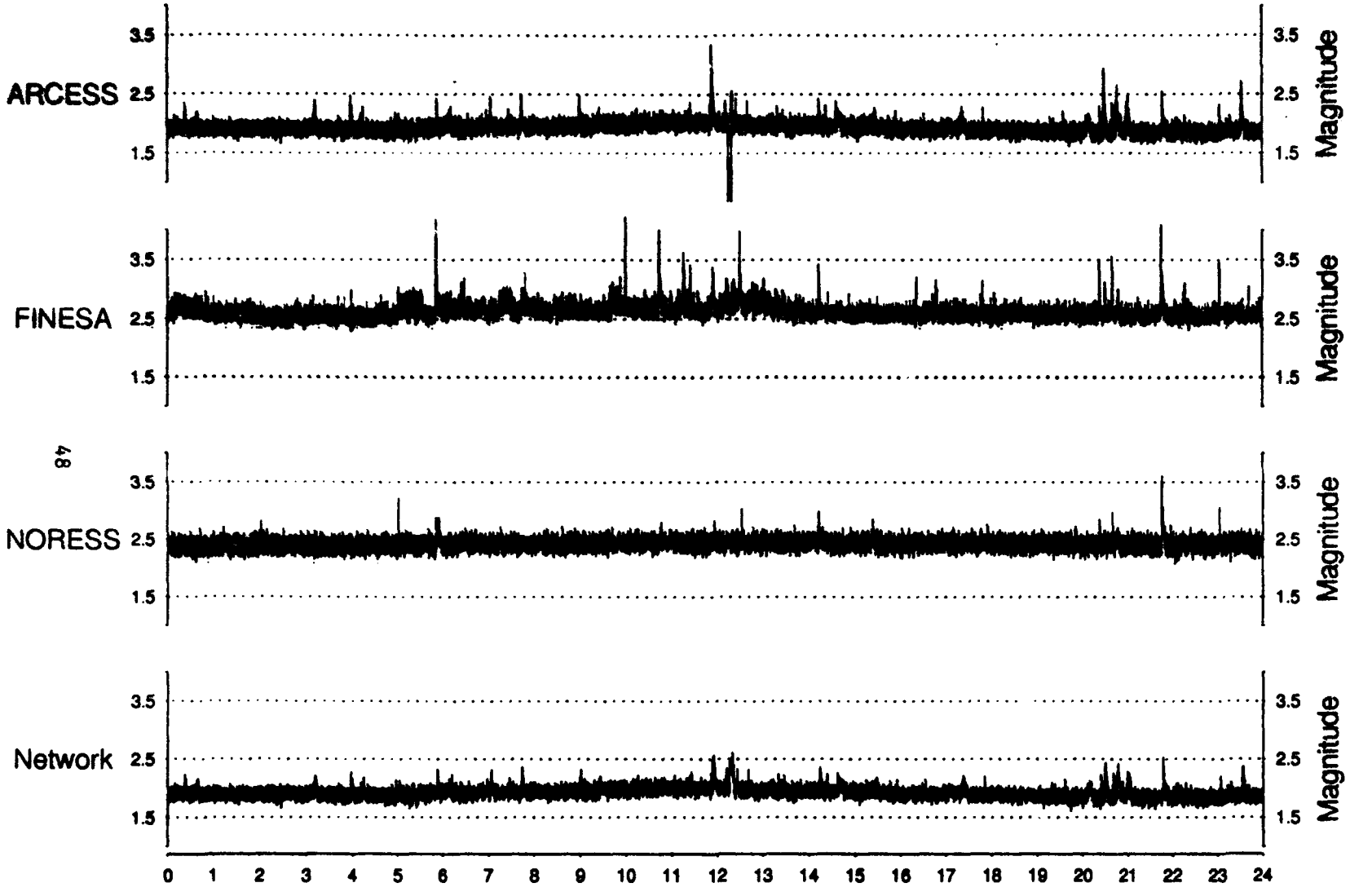
ARCESS
FINESA
NORESS
Network
3.5
2.5
1.5
Magnitude
0 1 2 3 4 5 6 7 8 9 10 11 12 13 14 15 16 17 18 19 20 21 22 23 24
Hours (GMT)
February 29, 1992

FIGURE A-29

DISTRIBUTION LIST

Prof. Thomas Ahrens
Seismological Lab, 252-21
Division of Geological & Planetary Sciences
California Institute of Technology
Pasadena, CA 91125

Prof. Keiiti Aki
Center for Earth Sciences
University of Southern California
University Park
Los Angeles, CA 90089-0741

Prof. Shelton Alexander
Geosciences Department
403 Deike Building
The Pennsylvania State University
University Park, PA 16802

Dr. Ralph Alewine, III
DARPA/NMRO
3701 North Fairfax Drive
Arlington, VA 22203-1714

Prof. Charles B. Archambeau
CIRES
University of Colorado
Boulder, CO 80309

Dr. Thomas C. Bache, Jr.
Science Applications Int'l Corp.
10260 Campus Point Drive
San Diego, CA 92121 (2 copies)

Prof. Muawia Barazangi
Institute for the Study of the Continent
Cornell University
Ithaca, NY 14853

Dr. Jeff Barker
Department of Geological Sciences
State University of New York
at Binghamton
Vestal, NY 13901

Dr. Douglas R. Baumgardt
ENSCO, Inc
5400 Port Royal Road
Springfield, VA 22151-2388

Dr. Susan Beck
Department of Geosciences
Building #77
University of Arizona
Tuscon, AZ 85721

Dr. T.J. Bennett
S-CUBED
A Division of Maxwell Laboratories
11800 Sunrise Valley Drive, Suite 1212
Reston, VA 22091

Dr. Robert Blandford
AFTAC/TT, Center for Seismic Studies
1300 North 17th Street
Suite 1450
Arlington, VA 22209-2308

Dr. G.A. Bollinger
Department of Geological Sciences
Virginia Polytechnical Institute
21044 Derring Hall
Blacksburg, VA 24061

Dr. Stephen Bratt
Center for Seismic Studies
1300 North 17th Street
Suite 1450
Arlington, VA 22209-2308

Dr. Lawrence Burdick
Woodward-Clyde Consultants
566 El Dorado Street
Pasadena, CA 91109-3245

Dr. Robert Burridge
Schlumberger-Doll Research Center
Old Quarry Road
Ridgefield, CT 06877

Dr. Jerry Carter
Center for Seismic Studies
1300 North 17th Street
Suite 1450
Arlington, VA 22209-2308

Dr. Eric Chael
Division 9241
Sandia Laboratory
Albuquerque, NM 87185

Prof. Vernon F. Cormier
Department of Geology & Geophysics
U-45, Room 207
University of Connecticut
Storrs, CT 06268

Prof. Steven Day
Department of Geological Sciences
San Diego State University
San Diego, CA 92182

Marvin Denny
U.S. Department of Energy
Office of Arms Control
Washington, DC 20585

Dr. Zoltan Der
ENSCO, Inc.
5400 Port Royal Road
Springfield, VA 22151-2388

Prof. Adam Dziewonski
Hoffman Laboratory, Harvard University
Dept. of Earth Atmos. & Planetary Sciences
20 Oxford Street
Cambridge, MA 02138

Prof. John Ebel
Department of Geology & Geophysics
Boston College
Chestnut Hill, MA 02167

Eric Fielding
SNEE Hall
INSTOC
Cornell University
Ithaca, NY 14853

Dr. Mark D. Fisk
Mission Research Corporation
735 State Street
P.O. Drawer 719
Santa Barbara, CA 93102

Prof Stanley Flatte
Applied Sciences Building
University of California, Santa Cruz
Santa Cruz, CA 95064

Dr. John Foley
NER-Geo Sciences
1100 Crown Colony Drive
Quincy, MA 02169

Prof. Donald Forsyth
Department of Geological Sciences
Brown University
Providence, RI 02912

Dr. Art Frankel
U.S. Geological Survey
922 National Center
Reston, VA 22092

Dr. Cliff Frolich
Institute of Geophysics
8701 North Mopac
Austin, TX 78759

Dr. Holly Given
IGPP, A-025
Scripps Institute of Oceanography
University of California, San Diego
La Jolla, CA 92093

Dr. Jeffrey W. Given
SAIC
10260 Campus Point Drive
San Diego, CA 92121

Dr. Dale Glover
Defense Intelligence Agency
ATTN: ODT-1B
Washington, DC 20301

Dr. Indra Gupta
Teledyne Geotech
314 Montgomery Street
Alexanderia, VA 22314

Dan N. Hagedon
Pacific Northwest Laboratories
Battelle Boulevard
Richland, WA 99352

Dr. James Hannon
Lawrence Livermore National Laboratory
P.O. Box 808
L-205
Livermore, CA 94550

Dr. Roger Hansen
HQ AFTAC/TTR
Patrick AFB, FL 32925-6001

Prof. David G. Harkrider
Seismological Laboratory
Division of Geological & Planetary Sciences
California Institute of Technology
Pasadena, CA 91125

Prof. Danny Harvey
CIRES
University of Colorado
Boulder, CO 80309

Prof. Donald V. Helmberger
Seismological Laboratory
Division of Geological & Planetary Sciences
California Institute of Technology
Pasadena, CA 91125

Prof. Eugene Herrin
Institute for the Study of Earth and Man
Geophysical Laboratory
Southern Methodist University
Dallas, TX 75275

Prof. Robert B. Herrmann
Department of Earth & Atmospheric Sciences
St. Louis University
St. Louis, MO 63156

Prof. Lane R. Johnson
Seismographic Station
University of California
Berkeley, CA 94720

Prof. Thomas H. Jordan
Department of Earth, Atmospheric &
Planetary Sciences
Massachusetts Institute of Technology
Cambridge, MA 02139

Prof. Alan Kafka
Department of Geology & Geophysics
Boston College
Chestnut Hill, MA 02167

Robert C. Kemerait
ENSCO, Inc.
445 Pineda Court
Melbourne, FL 32940

Dr. Max Koontz
U.S. Dept. of Energy/DP 5
Forrestal Building
1000 Independence Avenue
Washington, DC 20585

Dr. Richard LaCoss
MIT Lincoln Laboratory, M-200B
P.O. Box 73
Lexington, MA 02173-0073

Dr. Fred K. Lamb
University of Illinois at Urbana-Champaign
Department of Physics
1110 West Green Street
Urbana, IL 61801

Prof. Charles A. Langston
Geosciences Department
403 Deike Building
The Pennsylvania State University
University Park, PA 16802

Jim Lawson, Chief Geophysicist
Oklahoma Geological Survey
Oklahoma Geophysical Observatory
P.O. Box 8
Leonard, OK 74043-0008

Prof. Thorne Lay
Institute of Tectonics
Earth Science Board
University of California, Santa Cruz
Santa Cruz, CA 95064

Dr. William Leith
U.S. Geological Survey
Mail Stop 928
Reston, VA 22092

Mr. James F. Lewkowicz
Phillips Laboratory/GPEH
Hanscom AFB, MA 01731-5000(2 copies)

Mr. Alfred Lieberman
ACDA/VI-OA State Department Building
Room 5726
320-21st Street, NW
Washington, DC 20451

Prof. L. Timothy Long
School of Geophysical Sciences
Georgia Institute of Technology
Atlanta, GA 30332

Dr. Randolph Martin, III
New England Research, Inc.
76 Olcott Drive
White River Junction, VT 05001

Dr. Robert Masse
Denver Federal Building
Box 25046, Mail Stop 967
Denver, CO 80225

Dr. Gary McCartor
Department of Physics
Southern Methodist University
Dallas, TX 75275

Prof. Thomas V. McEvilly
Seismographic Station
University of California
Berkeley, CA 94720

Dr. Art McGarr
U.S. Geological Survey
Mail Stop 977
U.S. Geological Survey
Menlo Park, CA 94025

Dr. Keith L. McLaughlin
S-CUBED
A Division of Maxwell Laboratory
P.O. Box 1620
La Jolla, CA 92038-1620

Stephen Miller & Dr. Alexander Florence
SRI International
333 Ravenswood Avenue
Box AF 116
Menlo Park, CA 94025-3493

Prof. Bernard Minster
IGPP, A-025
Scripps Institute of Oceanography
University of California, San Diego
La Jolla, CA 92093

Prof. Brian J. Mitchell
Department of Earth & Atmospheric Sciences
St. Louis University
St. Louis, MO 63156

Mr. Jack Murphy
S-CUBED
A Division of Maxwell Laboratory
11800 Sunrise Valley Drive, Suite 1212
Reston, VA 22091 (2 Copies)

Dr. Keith K. Nakanishi
Lawrence Livermore National Laboratory
L-025
P.O. Box 808
Livermore, CA 94550

Dr. Carl Newton
Los Alamos National Laboratory
P.O. Box 1663
Mail Stop C335, Group ESS-3
Los Alamos, NM 87545

Dr. Bao Nguyen
HQ AFTAC/TTR
Patrick AFB, FL 32925-6001

Prof. John A. Orcutt
IGPP, A-025
Scripps Institute of Oceanography
University of California, San Diego
La Jolla, CA 92093

Prof. Jeffrey Park
Kline Geology Laboratory
P.O. Box 6666
New Haven, CT 06511-8130

Dr. Howard Patton
Lawrence Livermore National Laboratory
L-025
P.O. Box 808
Livermore, CA 94550

Dr. Frank Pilotte
HQ AFTAC/TT
Patrick AFB, FL 32925-6001

Dr. Jay J. Pulli
Radix Systems, Inc.
2 Taft Court, Suite 203
Rockville, MD 20850

Dr. Robert Reinke
ATTN: FCTVTD
Field Command
Defense Nuclear Agency
Kirtland AFB, NM 87115

Prof. Paul G. Richards
Lamont-Doherty Geological Observatory
of Columbia University
Palisades, NY 10964

Mr. Wilmer Rivers
Teledyne Geotech
314 Montgomery Street
Alexandria, VA 22314

Dr. George Rothe
HQ AFTAC/TTR
Patrick AFB, FL 32925-6001

Dr. Alan S. Ryall, Jr.
DARPA/NMRO
3701 North Fairfax Drive
Arlington, VA 22209-1714

Dr. Richard Sailor
TASC, Inc.
55 Walkers Brook Drive
Reading, MA 01867

Prof. Charles G. Sammis
Center for Earth Sciences
University of Southern California
University Park
Los Angeles, CA 90089-0741

Prof. Christopher H. Scholz
Lamont-Doherty Geological Observatory
of Columbia University
Palisades, CA 10964

Dr. Susan Schwartz
Institute of Tectonics
1156 High Street
Santa Cruz, CA 95064

Secretary of the Air Force
(SAFRD)
Washington, DC 20330

Office of the Secretary of Defense
DDR&E
Washington, DC 20330

Thomas J. Sereno, Jr.
Science Application Int'l Corp.
10260 Campus Point Drive
San Diego, CA 92121

Dr. Michael Shore
Defense Nuclear Agency/SPSS
6801 Telegraph Road
Alexandria, VA 22310

Dr. Matthew Sibol
Virginia Tech
Seismological Observatory
4044 Derring Hall
Blacksburg, VA 24061-0420

Prof. David G. Simpson
IRIS, Inc.
1616 North Fort Myer Drive
Suite 1440
Arlington, VA 22209

Donald L. Springer
Lawrence Livermore National Laboratory
L-025
P.O. Box 808
Livermore, CA 94550

Dr. Jeffrey Stevens
S-CUBED
A Division of Maxwell Laboratory
P.O. Box 1620
La Jolla, CA 92038-1620

Lt. Col. Jim Stobie
ATTN: AFOSR/NL
Bolling AFB
Washington, DC 20332-6448

Prof. Brian Stump
Institute for the Study of Earth & Man
Geophysical Laboratory
Southern Methodist University
Dallas, TX 75275

Prof. Jeremiah Sullivan
University of Illinois at Urbana-Champaign
Department of Physics
1110 West Green Street
Urbana, IL 61801

Prof. L. Sykes
Lamont-Doherty Geological Observatory
of Columbia University
Palisades, NY 10964

Dr. David Taylor
ENSCO, Inc.
445 Pineda Court
Melbourne, FL 32940

Dr. Steven R. Taylor
Los Alamos National Laboratory
P.O. Box 1663
Mail Stop C335
Los Alamos, NM 87545

Prof. Clifford Thurber
University of Wisconsin-Madison
Department of Geology & Geophysics
1215 West Dayton Street
Madison, WS 53706

Prof. M. Nafi Toksoz
Earth Resources Lab
Massachusetts Institute of Technology
42 Carleton Street
Cambridge, MA 02142

Dr. Larry Turnbull
CIA-OSWR/NED
Washington, DC 20505

Dr. Gregory van der Vink
IRIS, Inc.
1616 North Fort Myer Drive
Suite 1440
Arlington, VA 22209

Dr. Karl Veith
EG&G
5211 Auth Road
Suite 240
Suitland, MD 20746

Prof. Terry C. Wallace
Department of Geosciences
Building #77
University of Arizona
Tuscon, AZ 85721

Dr. Thomas Weaver
Los Alamos National Laboratory
P.O. Box 1663
Mail Stop C335
Los Alamos, NM 87545

Dr. William Wortman
Mission Research Corporation
8560 Cinderbed Road
Suite 700
Newington, VA 22122

Prof. Francis T. Wu
Department of Geological Sciences
State University of New York
at Binghamton
Vestal, NY 13901

AFTAC/CA
(STINFO)
Patrick AFB, FL 32925-6001

DARPA/PM
3701 North Fairfax Drive
Arlington, VA 22203-1714

DARPA/RMO/RETRIEVAL
3701 North Fairfax Drive
Arlington, VA 22203-1714

DARPA/RMO/SECURITY OFFICE
3701 North Fairfax Drive
Arlington, VA 22203-1714

HQ DNA
ATTN: Technical Library
Washington, DC 20305

Defense Intelligence Agency
Directorate for Scientific & Technical Intelligence
ATTN: DTIB
Washington, DC 20340-6158

Defense Technical Information Center
Cameron Station
Alexandria, VA 22314 (2 Copies)

TACTEC
Battelle Memorial Institute
505 King Avenue
Columbus, OH 43201 (Final Report)

Phillips Laboratory
ATTN: XPG
Hanscom AFB, MA 01731-5000

Phillips Laboratory
ATTN: GPE
Hanscom AFB, MA 01731-5000

Phillips Laboratory
ATTN: TSML
Hanscom AFB, MA 01731-5000

Phillips Laboratory
ATTN: SUL
Kirtland, NM 87117 (2 copies)

Dr. Michel Bouchon
I.R.I.G.M.-B.P. 68
38402 St. Martin D'Heres
Cedex, FRANCE

Dr. Michel Campillo
Observatoire de Grenoble
I.R.I.G.M.-B.P. 53
38041 Grenoble, FRANCE

Dr. Kin Yip Chun
Geophysics Division
Physics Department
University of Toronto
Ontario, CANADA

Prof. Hans-Peter Harjes
Institute for Geophysic
Ruhr University/Bochum
P.O. Box 102148
4630 Bochum 1, GERMANY

Prof. Eystein Husebye
NTNF/NORSAR
P.O. Box 51
N-2007 Kjeller, NORWAY

David Jepsen
Acting Head, Nuclear Monitoring Section
Bureau of Mineral Resources
Geology and Geophysics
G.P.O. Box 378, Canberra, AUSTRALIA

Ms. Eva Johannisson
Senior Research Officer
National Defense Research Inst.
P.O. Box 27322
S-102 54 Stockholm, SWEDEN

Dr. Peter Marshall
Procurement Executive
Ministry of Defense
Blacknest, Brimpton
Reading FG7-FRS, UNITED KINGDOM

Dr. Bernard Massinon, Dr. Pierre Mechler
Societe Radiomana
27 rue Claude Bernard
75005 Paris, FRANCE (2 Copies)

Dr. Svein Mykkeltveit
NTNT/NORSAR
P.O. Box 51
N-2007 Kjeller, NORWAY (3 Copies)

Prof. Keith Priestley
University of Cambridge
Bullard Labs, Dept. of Earth Sciences
Madingley Rise, Madingley Road
Cambridge CB3 OEZ, ENGLAND

Dr. Jorg Schlittenhardt
Federal Institute for Geosciences & Nat'l Res.
Postfach 510153
D-3000 Hannover 51, GERMANY

Dr. Johannes Schweitzer
Institute of Geophysics
Ruhr University/Bochum
P.O. Box 1102148
4360 Bochum 1, GERMANY